Response of "The Important Contribution of Secondary Formation and Biomass Burning to Oxidized Organic Nitrogen (OON) in a Polluted Urban Area: Insights from In Situ FIGAERO-CIMS Measurements" in *Atmos. Chem. Phys. Discuss. Doi: 10.5194/acp-2023-8*

Anonymous Referee #1

1.0. This study deploys an AMS and a FIGAERO-CIMS to investigate the sources and formation mechanisms of oxidized organic nitrogen (OON) species in an urban site in Guangzhou, China. By applying a tracer based method to FIGAERO-CIMS measurement, the contributions from biomass burning and secondary production to OON have been quantified. Further, the production rate of secondary OON is estimated based on the measured VOCs concentrations and literature values of ON yields. Overall, this study presents an interesting dataset and conducts comprehensive analysis. It improves our understanding of the concentration and speciation of OON in diverse environments. However, the conclusions on the source apportionment and formation mechanisms of OON are speculative as outlined below. I recommend accept with major revisions noted.

A1.0: We greatly appreciate the reviewer providing the valuable comments and constructive suggestions which help us tremendously in improving the quality of our work. All the responses to the specific comments are shown below. To facilitate the review process, we have copied the reviewer comments in black text. Our responses are in regular blue font. We have responded to all the referee comments and made alterations to our paper **(in bold text).**

Major Comments

1.1. The mass closure analysis on particle OON measured by CIMS and by AMS is valuable. It is shown that pOrgNO3,CIMS only accounts for ~30% of pOrgNO3,AMS (Line 228). In other words, CIMS only captures a small fraction of total pON, if the AMS measurement is reliable. Thus, the majority of the analysis in this study only focuses on a small fraction of total ON. A more important question is what the rest 70% of particle OON are. The reviewer understands this question is beyond the scope of this study, but this measurement limitation should be stressed more throughout the manuscript, to avoid the fallacy that the OON measured by I- CIMS, such as figure 7, represents the composition of all OON in the atmosphere. Similarly, the conclusions like half of particle OON originates from

biomass burning and the rest from secondary production should be discussed under the frame that the OON measured by I- CIMS are considered in the calculation, not total OON in the atmosphere.

A1.1: We agree with the reviewer's comment that the source apportionment results from CIMS cannot represent all the particle- and gas-phase OON in the ambient air. We stressed the measurement limitation of the CIMS throughout the revised main manuscript by emphasizing the OON reported here was mainly applicable to CIMS measurement and the OON mass detected by CIMS only accounted for 30% of values by AMS. For examples:

Line 375-377: **"On average, biomass burning emissions accounted for 49 ± 23% of total pOON measured by the CIMS, while the contribution was much lower (24 ± 25%) for gOON (Figs. 2b and 2d), indicating that biomass burning is one of the major sources for pOON measured by the CIMS, and gOON is predominately from secondary formation (76 ± 25%) (Huang et al., 2019; Lee et al., 2016)."**

Line 496-497: **"In this section, the molecular components of the gOON and pOON measured by the CIMS categorized with different oxygen and carbon atom numbers are briefly discussed."**

Line 534-535: **"Note that the sources of the undetected pOON from CIMS are still unknown, which shall be further investigated."**

Please also note that although the pOON measured by the CIMS only accounts for ~30% of the mass loading measured from AMS, we found that the measured pOON from two techniques correlated well, suggesting the rest of ~70% of mass from CIMS may have similar variation. Per reviewer #2's comments, we also calculated the potential uncertainty of measured pOON between CIMS and AMS. We found that the $pOrgNO_{3,CIMS}$ accounted for 28 ± 18% of $pOrgNO_{3,AMS}$ combined with uncertainty analysis in the revised Text S3 in supporting in formation. The detailed calculation can be found in A2.5.

1.2. Using C6H10O5I- as a tracer for biomass burning is not adequately justified. A major piece of evidence that biomass burning contributes to OON is figure 2a and 2c, which show the relationship between OON and C6H10O5I- is bifurcated. However, the same relationship is not observed between OON and other BB tracers including AMS mz60, methoxyphenol, and vanillic aicd. The contrasting observations are suspicious. The manuscript claims that BB tracers other than levoglucosan have all sorts of issues, such as non-biomass burning emissions, low concentration, or larger background. These issues could certainly be true. However, an obvious issue with C6H10O5I- is that it is not solely levoglucosan, but has interference from other isomers! Thus, it can be easily argued that C6H10O5I- is not a perfect tracer either. One should not rely the analysis solely on this single chemical formula. Let's imagine, among all the

CIMS ions, one ion, which is a tracer for VCP for example, exhibits similar correlation relationship with OON as C6H10O5 does (i.e., bifurcation as in Figure 2a). Then, the conclusion will easily become that VCP is a large contributor to OON. In conclusion, more evidence is required to support the contribution of biomass burning to OON. The authors mentioned that there are some episodes when pOON and levoglucosan peak coincidently (Figures S11a and S12a). Again, the figures only show pOON has some relationship with C6H10O5I-, not with levoglucosan, because the C6H10O5I- could be some other isomers.

A1.2: As the reviewer mentioned that the formula $C_6H_{10}O_5$ consisted of isomers in ambient atmosphere, which are levoglucosan, mannosan, and galactosan. In the same campaign, we also measured the isomer of levoglucosan based on filter sampling analyzed by high performance anion exchange chromatography with pulsed amperometric detection (HPAEC-PAD) (Zhang et al. 2015). The detailed information about this measurement can be found in recently published paper of Jiang et al. (2023) in the Science of Total Environment journal. The isomer measurement showed that the levoglucosan contributed 90 ± 2% of the total mass loading from three isomers of $C_6H_{10}O_5$ (Fig. A1) through the campaign, which was consistent with the previously reported results across China (80−95%) (Mao et al., 2018; Ho et al., 2014; Müller et al., 2023; Wang et al., 2018; Zhu et al., 2020).

Furthermore, we added measured results of potassium (K^+) to verify the source of $C_6H_{10}O_5$. K^+ can be treated as a tracer for biomass burning (Wang et al., 2017; Andreae, 1983) and is detected using IC based on filter sampling. The consistent variation of potassium (K^+) and levoglucosan supported that the enhancement of $C_6H_{10}O_5$ at high mass concentration shall mainly come from biomass burning (Wang et al., 2017), as shown in the reproduced Fig. S11a below.

To clarify this, we added corresponding information and revised the description in line 179-183 in the maintext as below. To be more precise and avoid confusion, we also updated all the compound name "**levoglucosan**" to be "**$C_6H_{10}O_5$**" or "**$C_6H_{10}O_5$ (levoglucosan and its isomers)**" when CIMS measurement was referred to in the manuscript. The uncertainty of using $C_6H_{10}O_5$ as tracer for biomass burning source apportionment of OON was also added, the detailed information can be found in A2.10.

"In the ambient air, the $C_6H_{10}O_5$ measured in the particle phase using the CIMS was probably composed by levoglucosan and its isomers (mannosan and galactosan) (Ye et al., 2021). The isomer measurement of $C_6H_{10}O_5$ in this campaign have revealed that the levoglucosan contributed 90 ± 2% mass loading of the three isomers of $C_6H_{10}O_5$ (Jiang et al., 2023), thus the $C_6H_{10}O_5$ signal in this study can be used as a tracer for biomass burning

emission (Bhattarai et al., 2019). The good correlation (R=0.78) between $C_6H_{10}O_5$ and another biomass burning tracer potassium (K^+) (Wang et al., 2017; Andreae, 1983), also supports this statement (Fig. S11a)."

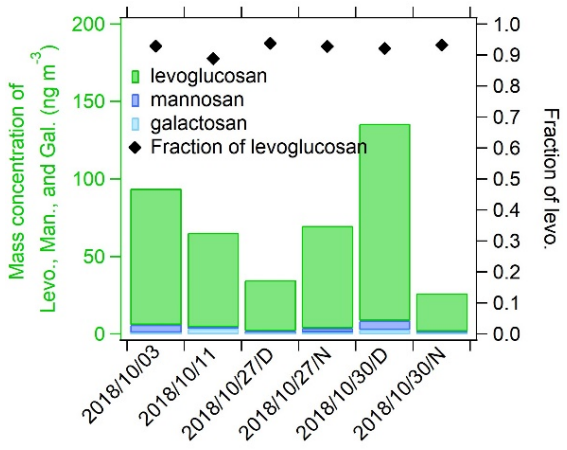

Figure A1. The mass concentration of $C_6H_{10}O_5$ isomers, i.e., levoglucosan, mannosan, and galactosan in this campaign. The mass fraction of levoglucosan to total $C_6H_{10}O_5$ isomer mass loading is also shown.

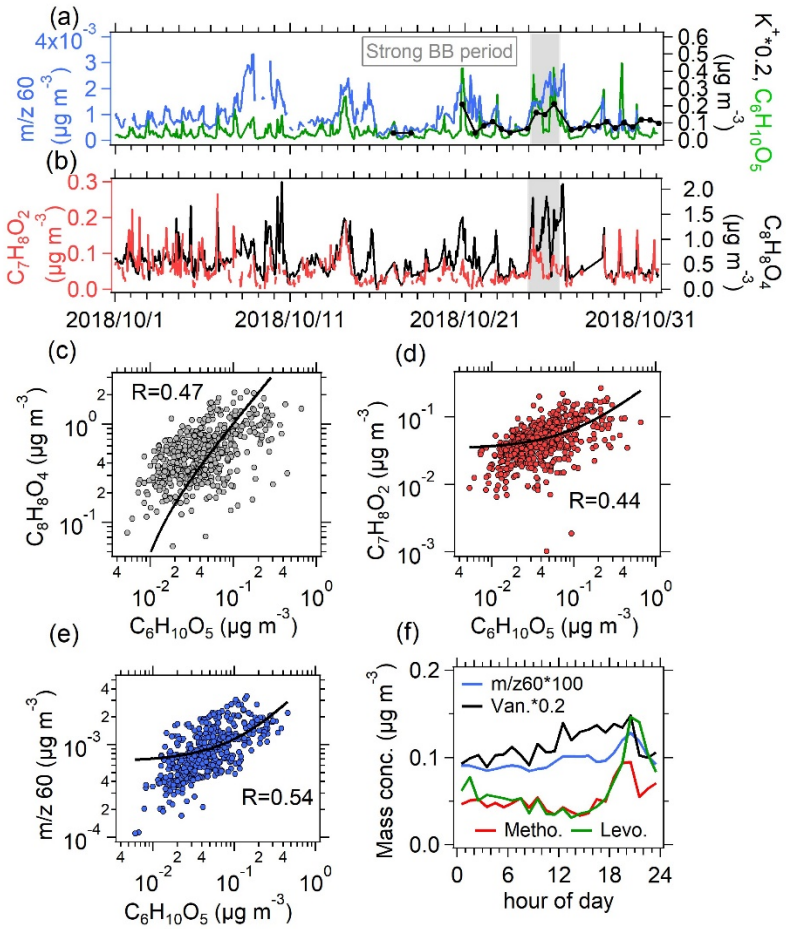

Figure S11. (a) Time series of *m/z* 60 from the AMS, particulate $C_6H_{10}O_5$ (levoglucosan and its isomers), water-soluble potassium (K^+), (b) $C_7H_8O_2$ (methoxyphenol and its isomers) and $C_7H_8O_2$ (methoxyphenol and its isomers) from CIMS. The *m/z* 60 was found to be a fragment from levoglucosan-like species and supposed to

be a tracer of biomass burning (Cubison et al., 2011). Scatter plots of (c) $C_7H_8O_2$ (methoxyphenol and its isomers), (d) $C_8H_8O_4$ (vanillic acid and its isomers), and (e) *m/z* 60 versus levoglucosan. Moderate agreement between them and $C_6H_{10}O_5$ also demonstrates the existence of biomass burning emissions (Urban et al., 2012). (f) Diurnal variation of the four species.

1.3. The production rate of secondary OON is estimated based on measured VOCs, but the usefulness of this analysis is limited. First, as the OON concentration depends on both production and loss, which is clearly pointed out in Line 369-371, the correlation between OON concentration and product rate is not very meaningful. As a result, there is no clear correlation between two terms as shown in this study. Second, the calculated production rate is not tied to the I CIMS measurement, which degrades the importance of such analysis. In other words, both methods do not validate each other. But it is at the authors' discretion regarding whether to keep this analysis.

A1.3: The production rate of OON was widely applied to investigate the formation pathway and potential contribution of VOCs to OON (Rollins et al., 2012; Liebmann et al., 2019; Sobanski et al., 2017; Ayres et al., 2015; Perring et al., 2013; Hamilton et al., 2021; Pye et al., 2015). It is true that the production rate did not account for the loss of OON results, however, to properly simulate the ambient OON concentration need modeling work with detailed mechanism account for the extra loss pathways including oxidation, photolysis, hydrolysis and deposition. The model simulation on mass concentration of OON in urban areas is still a challenge due to the complex formation and loss way of anthropogenic-derived OON (Li et al., 2023), which is beyond the scope of this manuscript. Under such background, the production rate calculation itself would be very meaningful to explore the formation mechanism of OON in urban areas in preliminary. In this study, we estimated the ambient mass concentration of NO_3 radicals based direct measurement of N_2O_5 by CIMS and obtained the time series of OH mass concentration using MCM model constrained by real J-value measurement. The detection of VOCs was also validated with multiple techniques. Overall, the dataset used for production rate estimation here is in high quality. Considering the uncertainty in both measurement of secondary gOON by CIMS and estimation of OON production rate, their similar diurnal variations show good agreement, which also supports the reasonability of the production rate calculated here. The rate production results give a summarized overview for the OON formation pathways and help us to better understand the future focus of OON studies. E.g., through OON production rate calculation, we found important OON formation through NO_3 pathways during the daytime, which highlight the potential contribution of NO_3 oxidation to other secondary products, e.g., SOA . The important contribution from monoterpene oxidation to OON was also revealed. Thus, we would like to keep these results and believe it is a very important part of our study. Finally, we revised the sentences in line 414-417 to remind the readers the potential uncertainty of production rate calculation in the maintext:

"To further elucidate the secondary formation mechanism of gOON, the diurnal patterns of gOON production rates from the three pathways following the procedure mentioned in section 2.3 are calculated and shown in Fig. 4a and Fig. S21. Although the production rate did not consider the loss of OON, the calculation of production rate still serves as a useful tool to assess the formation pathway and precursor contribution to OON (Liebmann et al., 2019; Sobanski et al., 2017; Hamilton et al., 2021)."

We also remind the readers that the life of pOON accounting for the loss of pOON shall be further investigated in the future in line 493-494:

"For the lifetime of pOON, a modeling study including explicit formation mechanism as conducted by Lee et al. (2016) is required for systematic explorations in the future."

1.4. Even though some analysis methods have been used in the literature, they still should be briefly explained to guide the readers who are not familiar with the methods. For example, Line 155 – 158 mentioned that three methods are applied to estimate the ON concentration based on AMS measurements. The basic principles behind each method should be briefly discussed (i.e., one or two sentences). For example, the NO2+/NO+ ratio method is based on the fact that inorganic and organic nitrates have different fragmentation patterns. Another examples include Line 232 and seasonal decomposed analysis (Line 348). Please briefly discuss the methods. Lastly, Line 431, please explain how the lifetime of gON is estimated.

A1.4: The detailed description of the three methods that were applied to estimate the ON concentration was already presented in detail in section 1 of the supporting information, where the principle of three ON estimation methods based on AMS measurement and the calculation process were fully addressed. Per the reviewer's comment, we also added brief description of each method in the revised main text in line 195-201:

"In addition to the total organic aerosol (OA), the mass concentration of $-ONO_2$ group from pON ($pOrgNO_{3,AMS}$) was also estimated by NO_2^+/NO^+ ratio method (Farmer et al., 2010; Fry et al., 2013; Day et al., 2022; Xu et al., 2015), positive matrix factorization (PMF) method (Hao et al., 2014), and thermodenuder (TD) method (Xu et al., 2021b) based on the AMS data. The NO_2^+/NO^+ ratio method was based on the different ratios of NO_2^+ to NO^+ fragmented from $pOrgNO_{3,AMS}$ and inorganic nitrate. The PMF method was performed by including the NO^+ and NO_2^+ ions into the PMF analysis combined with spectral matrix of organic ions. The TD method was conducted based on the difference of volatility between $pOrgNO_{3,AMS}$ and inorganic nitrates in particles."

The revised explanation of seasonal decomposed analysis can refer to Text S4 in supporting information manuscript. We also added brief description of the method and revised the sentence in the revised main text in line 400-403:

"To elucidate this large uncertainty, a seasonal decomposition method (Hilas et al., 2006), which was performed by locally weighted linear regression to decompose the time series into three components, i.e., trend component, seasonal component and remainder, was applied (detailed process can be found in Text S4). By replacing seasonal variation with hour variation, the method can down weight the impact of daily peak intensity variation."

We revised the estimation method of the lifetime of gOON in the last paragraph of section 3.3 (line 487-489):

"Furthermore, the lifetime of gOON in this study can be approximately estimated by a steady-state approach (gOON mixing ratio versus total production rate) as shown in Liebmann et al. (2019). A scatterplot of the secondary gOON versus the secondary gOON production rate at 1 hour time resolution is shown in Fig. S24b."

1.5. Issues regarding CIMS quantification. Does the calibration account for the temperature-dependence? A recent study shows that the I- CIMS sensitivity has a strong dependence on temperature[1]. This issue could be significant for particle-phase measurements, which have a higher IMR temperature. Line 134 mentioned that a voltage scanning procedure was used to estimate the sensitivity. However, neither detailed procedures nor calibration results are shown. Please describe the procedure, show the calibration curves, and show the accuracy of this method to the 39 compounds calibrated with authentic standards. Please discuss how the calibration curve is applied to estimate the sensitivity of individual compounds. Also, two recent studies have quantified the uncertainty of the voltage scanning method[2, 3], which should be cited and discussed in the manuscript.

A1.5: We thank the reviewer for his/her comments and suggestions. We maintained the IMR temperature in a stable condition by keeping heater strip and room temperature constant, as well as adding an insulation layer outside of the gas sampling line. The temperature of the IMR during measurement was kept almost constant (80 **℃)** to minimize the effect of temperature on sensitivity throughout the experiment set up. Thus, we think the temperature-dependent sensitivity shall be minor in this study. To clarify this, we added relative description in line 127-131 in the revised main text:

"The temperature of the IMR was kept almost constant by setting the temperature constant (80 ℃) of the heater strip in the IMR. Meanwhile, the room temperature, which was maintained by an air-conditioner, was

relatively stable (23.7 ± 2.9 °C). The gas sampling line inside the room was covered by heat insulation associated with a heating cable to hold the temperature of sampling gas steady. These protocols reduce the effect of the temperature dependence of IMR, as indicated by Robinson et al. (2022) that I^- CIMS sensitivity may be influenced by the temperature of IMR."

The detail description of the calibration experiments and data processing in this campaign, e.g., voltage scanning, was already shown in a previous paper of Ye et al. (2021) (copied as Fig. A2 below). We added a brief description on the calibration method about voltage scanning method and how the calibration curve was applied to estimate the sensitivity of individual compound in line 148-160 in the maintext:

" Lopez-Hilfiker et al. (2016) and Iyer et al. (2016) have verified the connections among the binding energy of the iodide-adduct bond, the voltage dissociating iodide adducts and the sensitivity of corresponding species. The relationship between the voltage difference (*dV*) and signal fraction remaining of an iodide-molecule adduct is established by scanning the *dV* between the skimmer of the first quadrupole and the entrance to the second quadrupole ion guide of the mass spectrometer. This relationship curve of an individual iodide adduct can be fitted by a sigmoid function and yields two parameters: S_0, the relative signal at the weakest *dV* compared to the signal under operational *dV*; dV_{50}, the voltage at which half of the maximum signal is removed (i.e., half the adducts that could be formed are de-clustered). A sigmoidal fit was then applied to the results of all the iodide adducts. An empirical relationship between relative sensitivity ($1/S_0$) and dV_{50} of each ion (includes levoglucosan) based on average values of the entire campaign was obtained. By linking the relative sensitivity of levoglucosan with its absolute sensitivity based on the authentic standard, the absolute sensitivity of all the uncalibrated OON species was determined, after taking into account the relative transmission efficient of all the ions. The detailed data of these response factors can be found in the supporting information of Ye et al. (2021)."

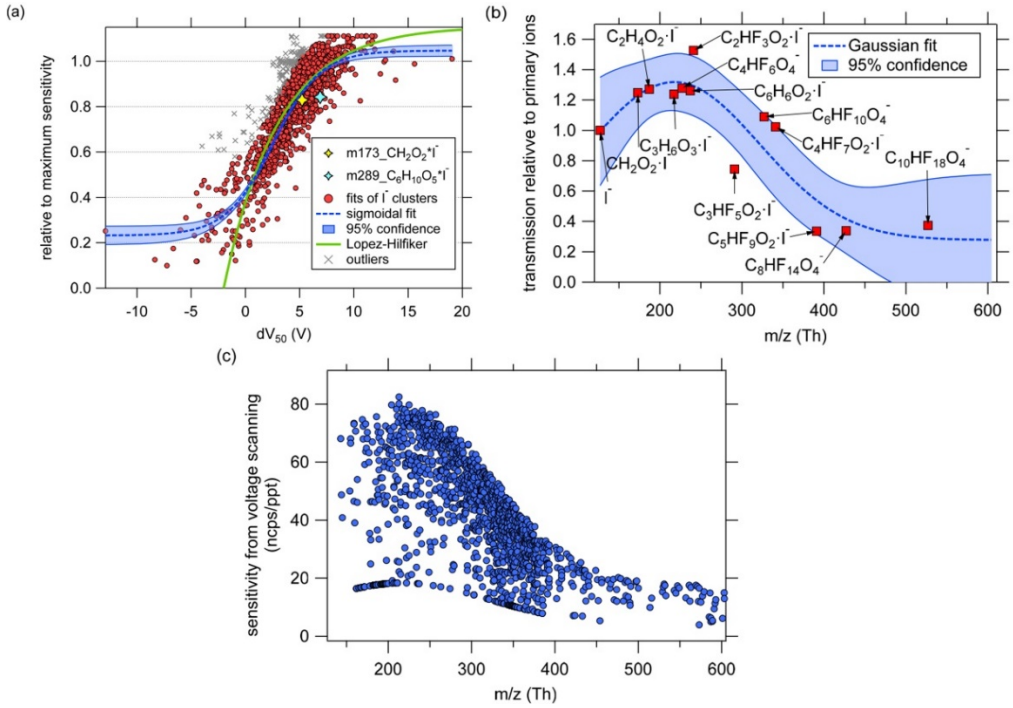

"Figure A2. The original Figure S7 in the supporting information of Ye et al. 2021. (a) Fitting the voltage scanning results as a sigmoidal function of sensitivity relative to maximum sensitivity versus dV_{50} (i.e., the voltage where half of an iodide adducts dissociate). (b) Fitting relative transmission efficiency as a gaussian curve of m/z. (c) The sensitivity derived from voltage scanning procedure. The transmission correction has been applied. The bottom line in Figure A2c that has a shape exactly the same as the transmission curve represents the points with a cutoff of 0.23 for the relative sensitivity."

The uncertainty of voltage scanning method was quantified in previous studies including two studies mentioned by the reviewer and Isaacman-Vanwertz et al. (2018). This approach was found to carry high uncertainties for individual analytes (0.5 to 1 order of magnitude) but represent a central tendency that can be used to estimate the sum of analytes with reasonable error (~30% differences between predicted and measured moles) (Bi et al., 2021b). Based on the analysis of the uncertainties of three nitrogen-containing compounds (in the list of calibrated species) derived both from the voltage scanning method and the method using the standard compounds, we approximately obtained 32–56% underestimation of sensitivity for the voltage scanning method. Through the comparison of the sensitivity factors derived from the two methods is added in Figure S3 (also shown as below), an average value of 47% was regarded as the uncertainty of the voltage scanning method and the total mass loading of uncalibrated species. To clarify this, we added the description of uncertainty analysis of the voltage scanning method in line 160-168:

"Three OON species which are 4-nitrophenol ($C_6H_5NO_3$), 2,4-dinitrophenol ($C_6H_4N_2O_5$), and 4-nitrocatechol ($C_6H_5NO_4$) were calibrated in both authentic standards and voltage scanning methods. By comparing their sensitivity (Fig. S3), the uncertainty of the voltage scanning method can be roughly estimated. Detailed description of the calibration curves and the application of the calibration curve to estimate the sensitivity can

be referred to the supporting information text of Ye et al. (2021). In general, the voltage scanning method underestimates (32−56%) the sensitivity of OON in this study compared to the values using the standard compounds as real. This uncertainty was comparable with 30% uncertainty of all analytes in Bi et al. (2021b) and 60% uncertainty of total carbon in Isaacman-Vanwertz et al. (2018) measured by the Iodide-CIMS. Finally, an avergae underestimation of 47% on sensitivity was taken as the uncertainty of the whole OON mass loading in this study."

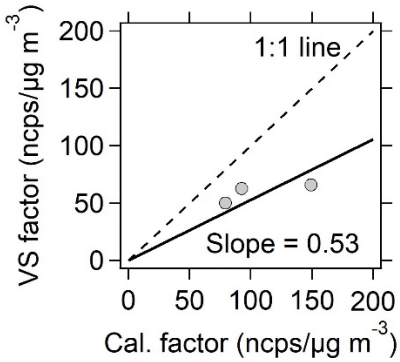

Figure S3. The scatterplot of calibration factors of three nitro-containing compounds (4-nitrophenol, 2,4-dinitrophenol, and 4-nitrocatechol) that derived from voltage scanning method and standard calibration. Based on the slope, 47% was regarded as the uncertainty of the voltage scanning method for OON calibration in this study. The detailed data can be found in the excel file of the supplement zip package of Ye et al. (2021).

Minor Comments

1.6. Lines 50 and 78. Please cite Xu et al. 2015 ACP4 which also extensively discussed the NO2+/NO+ ratio method.

A1.6: In fact, the paper Xu et al. 2015 ACP was already cited in line 204 in the original main text and also in Text S1 in the supporting information. After checking through the manuscript, we also added the citation of Xu et al. 2015 ACP in Line 50, line 78 and line 194 in the revised main text:

In line 50: **"(II) by using aerosol mass spectrometer (AMS) (Decarlo et al., 2006) based on NO_2^+/NO^+ apportionment (Farmer et al., 2010; Fry et al., 2013; Hao et al., 2014; Day et al., 2022; Xu et al., 2015) and/or thermodenuder (Xu et al., 2021b);"**

In line 78: **"Previous studies indicated that the oxidation of biogenic VOCs by NO_3 dominated gOON formation at a forest-urban site in Germany (56% of average gOON production rate) (Sobanski et al., 2017), as well as at a boreal forest site in the Finland (70% of total gOON production rate) (Liebmann et al., 2019) and the southeast US (84% of monoterpene organic nitrate mass) (Ayres et al., 2015; Pye et al., 2015; Xu et al., 2015)."**

In line 197: **"In addition to the total organic aerosol (OA), the mass concentration of $-ONO_2$ group from pON ($pOrgNO_{3,\ AMS}$) was also estimated by NO_2^+/NO^+ ratio method (Farmer et al., 2010; Fry et al., 2013; Day et al., 2022; Xu et al., 2015),"**

1.7. Line 60. Please cite Chen et al. 2020 ACP5 which also deployed FIGAERO-CIMS to measure organic nitrates. Please also discuss Chen et al. in related analysis, such as the comparison between AMS and FIGAERO-CIMS.

A1.7: We thank the reviewer for the reminding. We have read attentively through the paper of Chen et al. 2020 ACP, then added the citation of Chen et al. (2020) in the corresponding sentence in line 61 and in the overview of pON/OA in Fig. S7 as shown below.

"So far, gOON and pOON (containing 4–12 oxygen atoms) formed from multiple oxidation process of volatile organic compounds (VOCs) have been quantified by a high-resolution time-of-flight CIMS installed with a Filter Inlet for Gases and AEROsols (FIGAERO-CIMS) in the forests (Lee et al., 2018; Lee et al., 2016) and at rural sites (Huang et al., 2019; Chen et al., 2020)."

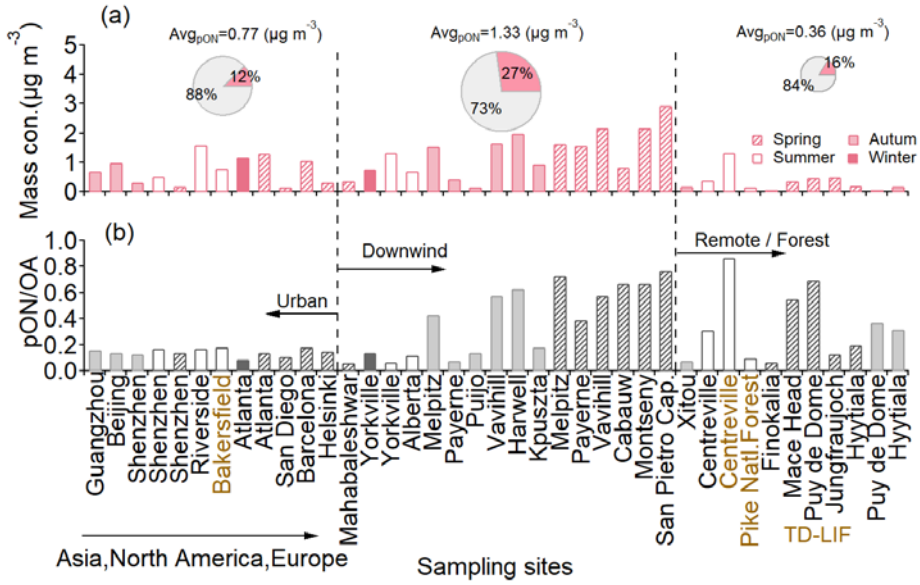

Figure S7. (a) Mass concentration pON and (b) its fraction to OA at sites around the world (Ayres et al., 2015; Chen et al., 2020; Day et al., 2010; Farmer et al., 2010; Fisher et al., 2016; Fry et al., 2013; Kiendler-Scharr et al., 2016; Lanz et al., 2010; Lee et al., 2019; Rollins et al., 2012; Salvador et al., 2020; Singla et al., 2019; Xu et al., 2015; Yu et al., 2019) classified into urban sites, downwind sites (lied downwind of the cities where were influenced by the emissions from the cities), forest or remote sites with different seasons. The average molecular weight of ON used for all sites is assumed to be 200 g mol^{-1}. The inset pies indicate the average fraction of pON

(pink) to OA at each type of site. The yellow indicates the data are measured by thermal dissociation laser-induced fluorescence instrument (TD-LIF). The method of the $pON_{AMS/TD-LIF}$/OA calculation was referred to Takeuchi and Ng (2019).

1.8. Line 125. Do all 339 compounds have signal significantly higher than the background? Or 339 refers to the number compounds that are fitted in the HR analysis?

A1.8: Yes, the 339 compounds were selected due to that they can be fitted in the HR analysis after subtracting the background. To clarify this, we revised the sentence in line 138-140.

"Based on the CIMS measurement, speciated OON (nitrogen-containing oxygenated hydrocarbons, 339 closed-shell compounds with oxygen versus carbon atom ratio no less than 3, $C_{\geq 1}H_{\geq 1}O_{\geq 3}N_{1-2}$) in both gas and particle phases were quantified. These OON compounds can be fitted well in the HR analysis after the background signals have been removed."

1.9. Line 200. The underlying assumption of this statement is unclear. Does the fraction of organic nitrate in total nitrate increases with decreasing OA concentration?

A1.9: We are sorry that we do not quite understand what the assumption that the reviewer refers to here. For the second question, the fraction of organic nitrate in total nitrate as a function of OA concentration was displayed in Fig. A3. The faction of ON in total nitrates decreases as a function of OA mass concentrations above 10 μg m^{-3}.

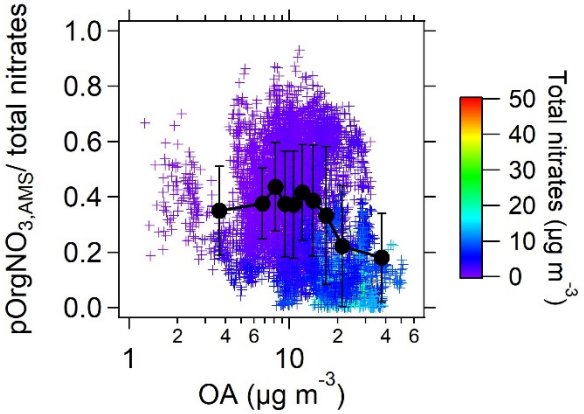

Figure A3. Mass fraction of $pOrgNO_{3,AMS}$ (NO_2^+/NO^+ ratio method) to total nitrates as a function of total OA derived from the AMS. The points are color-coded with total nitrates.

1.10. Line 225-228. There are many acronyms in this paragraph, including $pOON_{CIMS}$, $pOON_{AMS}$, $pOrgNO3_{CIMS}$, $pOrgNO3_{AMS}$. Please better explain the difference between these terms.

A1.10: To provide a comprehensive explanation of the acronyms, we added Table A1 in the appendix to explain all nomenclature mentioned in this manuscript:

"Appendices A: Summary of the acronym

Table A1. The summary of the acronym and corresponding full name in this study.

Acronym	Full name	Acronym	Full name
ALWC	aerosol liquid water content	ONs	organic nitrates
$C_{11-20}N$	oxidized organic nitrogen molecules with 11−20 carbon atoms	OON	oxidized organic nitrogen
$C_{4-5}N$	oxidized organic nitrogen molecules with 4−5 carbon atoms	OON_{bb}	oxidized organic nitrogen from biomass burning
$C_{6-9\ Aro}N$	oxidized organic nitrogen molecules with 6−9 carbon atoms and benzene ring	OON_{sec}	oxidized organic nitrogen from secondary formation
$C_{8-10}N$	oxidized organic nitrogen molecules with 8−10 carbon atoms	O_x	odd oxygen, sum of O_3 and NO_2
CHON	oxidized organic nitrogen with only one nitrogen atom	pC_xN	particle-phase C_xN
$CHON_2$	oxidized organic nitrogen with two nitrogen atoms	PMF	positive matrix factorization
CIMS	chemical ionization mass spectrometer	pON	particle-phase organic nitrates
$C_{others}N$	oxidized organic nitrogen molecules not in other four group	pOON	particle-phase oxidized organic nitrogen
C_xN	oxidized organic nitrogen molecules with x carbon atoms	$pOON_{AMS}$	particle-phase oxidized organic nitrogen derived from aerosol mass spectrometer measurement.
dV	voltage difference	$pOON_{CIMS}$	particle-phase oxidized organic nitrogen measured by chemical ionization mass spectrometer
dV_{50}	the voltage at which half the signal is removed (i.e., half of iodide adducts dissociate)	$pOrgNO_{3,\ AMS}$	Nitrate functional group from particle-phase OON measured by aerosol mass spectrometer
FIGAERO-I-CIMS	an iodide-adduct chemical ionization mass spectrometer equipped with a Filter Inlet for Gases and AEROsols	$pOrgNO_{3,CIMS}$	Nitrate functional group in particle-phase OON based on the data by chemical ionization mass spectrometer
GC-MS/FID	gas chromatography coupled with mass spectrometry and flame ionization detector	PRIDE-GBA	Particles, Radicals, and Intermediates from oxidation of primary Emissions over the Great Bay Area
gON	gas-phase organic nitrates	PTR-ToF-MS	proton transfer reaction time-of-flight mass spectrometry
gOON	gas-phase oxidized organic nitrogen	RH	relative humidity
$gOON_{CIMS}$	gas-phase oxidized organic nitrogen measured by chemical ionization mass spectrometer	S_0	the relative signal at weakest *dV* compared to the signal under operational *dV*
HR-ToF-AMS	high-resolution time-of-flight aerosol mass spectrometer	TD	thermodenuder
IMR	ion-molecule reaction region	TD-LIF	thermal dissociation laser induced fluorescence
MW	molecular weight	VCP	volatile chemical product
NO_x	Sum of NO and NO_2	VOCs	volatile organic compounds

"

1.11. Line 247-248. Please explain "high susceptibility influenced by temperature".

A1.11: We revised this sentence in line 293-295:

"The slightly poor correlation of $C_{4-5}N$ groups between gas and aerosol phase was probably caused by less partitioning of substantial formed isoprene-oxidized gOON in the daytime to the pOON compared to other long-chain compounds."

1.12. Line 253. "photolysis rate" in this sentence is confusing, because reader may think it refers to the photolysis rate of OON. Replace "photolysis rate" with jNO2 or solar radiation.

A1.12: "Photolysis rate" was replaced with "jNO_2" in line 300.

1.13. Line 258. It should be figure 1d, instead of figure 1f.

A1.13: Corrected (in line 305).

1.14. Line 282. replace "NO/NOx concentration" with "NO and NOx concentrations".

A1.14: Corrected (in line 330).

1.15. Line 312 and Text S4. If the reviewer understands correctly, the "seasonal decompose analysis" removes the seasonal variation from the diurnal variation. However, the data only include one-month measurement and it is not clear why this analysis is necessary. Also, text S4 does not clearly describe the method at all. This method section should be expanded.

A1.15: The "seasonal decompose analysis" is the original name of the method, which is always used to resolve long-term and repeated variation in term of years and seasonal variation. The two variation trends are similar to a combination of two filters with large and small bandwidth, which can be adjusted. Here we changed the "bandwidth" of the method by replacing seasonal variation with hour variation and replacing long-term variation in term of years with days. We reserved this expression of "seasonal decompose analysis" in the manuscript for its original application. To clarify this, we revised the sentence in line 400-403 of the main text:

"To elucidate this large uncertainty, a seasonal decomposition method (Hilas et al., 2006), which was performed by locally weighted linear regression to decompose the time series into three components, i.e., trend component, seasonal component and remainder, was applied (detailed process can be found in Text S4). By replacing

seasonal variation with hour variation, the method can down weight the impact of daily peak intensity variation."

In addition, we expanded the method section Text S4 in the supporting information to introduce more details about this method:

"A time series usually comprises three components: a long-term trend, seasonal fluctuation, and a remainder component (containing anything else in the time series). A long-term trend is a tendency or state of affairs in which a phenomenon develops and changes continuously over a longer period of time. Seasonal fluctuation is the regular variation caused by seasonal change. The time series decomposition can distill the component of repeatability from complex data. This method is similar to the combination of two filters with large and small bandwidth. The bandwidth can be adjusted for different time resolution. If an additive decomposition was assumed, the Eq. is:

$$y_t = S_t + T_t + R_t \quad \text{(S10)}$$

where y_t is the data, S_t is the seasonal fluctuation, T_t is the long-term trend, and R_t is the remainder component, all at period t. Taking 24 hours as the "season" in the calculation, i.e., adjusting the "bandwidth", we can get a clearer diurnal variation preventing the trend blurred by the varies intensity between days. The detailed process of the calculation applied in this paper can refer to Hilas et al. (2006)."

1.16. Line 340. For the strong BB emission period, are VOCs from BB considered in the calculation of OON production rate?

A1.16: The VOCs considered in the calculation of OON production rate are the same during the whole campaign, including the strong BB emission period here. VOCs from biomass burning emissions include alkanes, alkenes, aromatics (e.g., phenol and cresol), and terpenes (e.g., isoprene and monoterpenes) (Gilman et al. 2015;Liu et al. 2017). Thus, the calculation of OON production rate during the strong BB emission period shall include VOCs from biomass burning. To clarify this, we added brief discussion in line 370-372 of the main text:

"The precursors, e.g., alkanes, alkenes, aromatics (phenol and cresol), and terpenes (isoprene and monoterpenes), considered in the calculation were also contributed by biomass burning (Liu et al., 2017; Gilman et al., 2015), especially during the strong biomass burning emission period."

1.17. Line 413. Please rewrite this sentence because RO2+NO produces either RONO2 or O3.

A1.17: The sentence was revised in line 468-470:

"Fig. 6a shows a strong correlation between secondary gOON and O_x (R = 0.83, slope = 0.02 μg m^{-3}/ppb), which is within expectation as the major channel of gOON formation between peroxy radicals (RO_2) and NO can lead to the formation of ONs and O_3 by continual radical propagation and photolysis of NO_2 (Perring et al., 2013; Xu et al., 2021a)."

1.18. Figure S21. Please explain why ALWC (RH and others) is correlated with pOON/Ox, instead of pOON?

A1.18: The ALWC is correlated with "secondary pOON/O_x" ($pOON_{sec}/O_x$) as shown in Fig. S23 (original Fig. S21) in the revised supporting information. Using $pOON_{sec}/O_x$ instead of $pOON_{sec}$ was originated from Herndon et al. (2008) and Wood et al. (2010). Both studies showed that the observed [OOA]/[O_x] roughly serves as a useful tool to represent the calculated production of SOA vs production of O_x (P[SOA]/P[O_x]). As citated equation shown below:

$$\frac{\Delta[\mathrm{SOA}]}{\Delta[\mathrm{O_X}]} \approx \frac{P[\mathrm{SOA}]}{P[\mathrm{O_X}]}$$ (Wood et al., 2010)

In the recent studies, the variation of OOA/O_x ratios have been attributed to several factor including photochemical oxidation, heterogenous/aqueous reaction, and mixing with air aloft that contains residual SOA and O_x during boundary layer growth (Hu et al., 2016; Hayes et al., 2013; Nault et al., 2021). Nault et al. (2021) found the ratio of [OOA]/[O_x] is highly correlated with the BTEX fraction (Benzene, Toluene, Ethylbenzene and Xylene) in total measured VOCs among different urban areas across the world. Compared with short chain VOCs, the BTEX VOCs are more efficient to form SOA than O_x, resulting a higher OOA/O_x ratio. Multiple studies also found the OOA/O_x ratio also increases when there are heterogeneous/aqueous reactions which can lead to extra SOA formation but not O_x (Zhang et al., 2018; Zhan et al., 2021; Xu et al., 2017; Dai et al., 2019; Hu et al., 2016). In this study, we applied a similar concept of OOA/O_x to $pOON_{sec}/O_x$, since $pOON_{sec}$ is part of SOA.

The $pOON_{sec}/O_x$ ratios that positively correlated with ALWC and wet aerosol surface area suggested that the $pOON_{sec}$ formed by heterogenous/aqueous reaction partially account for the increasing ratio compared to gas-phase photochemistry (together with O_x formation). If absolute $pOON_{sec}$ instead of $pOON_{sec}/O_x$ was used, the correlation between RH (ALWC) and $pOON_{sec}$ would probably be influenced by meteorological factors (e.g., boundary layer height), introducing more ambiguity of the conclusion. Thus, the $pOON_{sec}/O_x$ instead of $pOON_{sec}$ was applied here. To clarify this, we added relative description and revised the caption of Figure S23:

"Figure S23. The ratio of Secondary (Sec.) pOON to Ox versus the (a) RH, (b) aerosol liquid water content (ALWC), (c) wet aerosol surface area, and (d) ambient temperature color-coded using the RH during the campaign. Regression slopes between pOON and Ox in photochemically processed urban emissions provide a metric to investigate the relative efficiency of pOON versus O_3 formation during photochemical oxidation (Wood et al., 2010; Hayes et al., 2013). The different values of secondary pOON/O_x ratio can be attributed to photochemical oxidation from different VOC constituent (Nault et al., 2021), heterogenous/aqueous reaction (Zhang et al., 2018; Zhan et al., 2021; Xu et al., 2017; Dai et al., 2019; Hu et al., 2016), and mixing with air aloft that contains residual pOON and O_x during boundary layer growth (Wood et al., 2010). The secondary pOON/O_x ratios that positive correlated with ALWC and wet aerosol surface area suggested that partial pOON might be formed by heterogenous/aqueous reaction, which can efficiently produce secondary pOON but inefficiently on O_x."

Reference

Andreae, M. O.: Soot Carbon and Excess Fine Potassium: Long-Range Transport of Combustion-Derived Aerosols, Science, 220, 1148-1151, https://doi.org/10.1126/science.220.4602.1148, 1983.

Ayres, B. R., Allen, H. M., Draper, D. C., Brown, S. S., Wild, R. J., Jimenez, J. L., Day, D. A., Campuzano-Jost, P., Hu, W., de Gouw, J., Koss, A., Cohen, R. C., Duffey, K. C., Romer, P., Baumann, K., Edgerton, E., Takahama, S., Thornton, J. A., Lee, B. H., Lopez-Hilfiker, F. D., Mohr, C., Wennberg, P. O., Nguyen, T. B., Teng, A., Goldstein, A. H., Olson, K., and Fry, J. L.: Organic nitrate aerosol formation via NO3+ biogenic volatile organic compounds in the southeastern United States, Atmos. Chem. Phys., 15, 13377-13392, https://doi.org/10.5194/acp-15-13377-2015, 2015.

Bhattarai, H., Saikawa, E., Wan, X., Zhu, H., Ram, K., Gao, S., Kang, S., Zhang, Q., Zhang, Y., Wu, G., Wang, X., Kawamura, K., Fu, P., and Cong, Z.: Levoglucosan as a tracer of biomass burning: Recent progress and perspectives, Atmospheric Research, 220, 20-33, https://doi.org/10.1016/j.atmosres.2019.01.004, 2019.

Bi, C., Krechmer, J. E., Frazier, G. O., Xu, W., Lambe, A. T., Claflin, M. S., Lerner, B. M., Jayne, J. T., Worsnop, D. R., Canagaratna, M. R., and Isaacman-VanWertz, G.: Coupling a gas chromatograph simultaneously to a flame ionization detector and chemical ionization mass spectrometer for isomer-resolved measurements of particle-phase organic compounds, Atmos. Meas. Tech., 14, 3895-3907, https://doi.org/10.5194/amt-14-3895-2021, 2021a.

Bi, C., Krechmer, J. E., Frazier, G. O., Xu, W., Lambe, A. T., Claflin, M. S., Lerner, B. M., Jayne, J. T., Worsnop, D. R., Canagaratna, M. R., and Isaacman-VanWertz, G.: Quantification of isomer-resolved iodide chemical ionization mass spectrometry sensitivity and uncertainty using a voltage-scanning approach, Atmos. Meas. Tech., 14, 6835-6850, https://doi.org/10.5194/amt-14-6835-2021, 2021b.

Chen, Y., Takeuchi, M., Nah, T., Xu, L., Canagaratna, M. R., Stark, H., Baumann, K., Canonaco, F., Prévôt, A. S. H., Huey, L. G., Weber, R. J., and Ng, N. L.: Chemical characterization of secondary organic aerosol at a rural site in the southeastern US: insights from simultaneous high-resolution time-of-flight aerosol mass spectrometer (HR-ToF-AMS) and FIGAERO chemical ionization mass spectrometer (CIMS) measurements, Atmos. Chem. Phys., 20, 8421-8440, https://doi.org/10.5194/acp-20-8421-2020, 2020.

Cubison, M. J., Ortega, A. M., Hayes, P. L., Farmer, D. K., Day, D., Lechner, M. J., Brune, W. H., Apel, E., Diskin, G. S., Fisher, J. A., Fuelberg, H. E., Hecobian, A., Knapp, D. J., Mikoviny, T., Riemer, D., Sachse, G. W., Sessions, W., Weber, R. J., Weinheimer, A. J., Wisthaler, A., and Jimenez, J. L.: Effects of aging on organic aerosol from open biomass burning smoke in aircraft and laboratory studies, Atmos. Chem. Phys., 11, 12049-12064, https://doi.org/10.5194/acp-11-12049-2011, 2011.

Dai, Q., Schulze, B. C., Bi, X., Bui, A. A. T., Guo, F., Wallace, H. W., Sanchez, N. P., Flynn, J. H., Lefer, B. L., Feng, Y., and Griffin, R. J.: Seasonal differences in formation processes of oxidized organic aerosol near Houston, TX, Atmos. Chem. Phys., 19, 9641-9661, 10.5194/acp-19-9641-2019, 2019.

Day, D. A., Liu, S., Russell, L. M., and Ziemann, P. J.: Organonitrate group concentrations in submicron particles with high nitrate and organic fractions in coastal southern California, Atmos. Environ., 44, 1970-1979, https://doi.org/10.1016/j.atmosenv.2010.02.045, 2010.

Day, D. A., Campuzano-Jost, P., Nault, B. A., Palm, B. B., Hu, W., Guo, H., Wooldridge, P. J., Cohen, R. C., Docherty, K. S., Huffman, J. A., de Sá, S. S., Martin, S. T., and Jimenez, J. L.: A systematic re-evaluation of methods for quantification of bulk particle-phase organic nitrates using real-time aerosol mass spectrometry, Atmos. Meas. Tech., 15, 459-483, https://doi.org/10.5194/amt-15-459-2022, 2022.

DeCarlo, P. F., Kimmel, J. R., Trimborn, A., Northway, M. J., Jayne, J. T., Aiken, A. C., Gonin, M., Fuhrer, K., Horvath, T., Docherty, K. S., Worsnop, D. R., and Jimenez, J. L.: Field-Deployable, High-Resolution, Time-of-Flight Aerosol Mass Spectrometer, Anal. Chem., 78, 8281-8289, https://doi.org/10.1021/ac061249n, 2006.

Farmer, D. K., Matsunaga, A., Docherty, K. S., Surratt, J. D., Seinfeld, J. H., Ziemann, P. J., and Jimenez, J. L.: Response of an aerosol mass spectrometer to organonitrates and organosulfates and implications for atmospheric chemistry, Proc. Natl. Acad. Sci. U. S. A., 107, 6670-6675, https://doi.org/10.1073/pnas.0912340107, 2010.

Fisher, J. A., Jacob, D. J., Travis, K. R., Kim, P. S., Marais, E. A., Miller, C. C., Yu, K., Zhu, L., Yantosca, R. M., Sulprizio, M. P., Mao, J., Wennberg, P. O., Crounse, J. D., Teng, A. P., Nguyen, T. B., St Clair, J. M., Cohen, R. C., Romer, P., Nault, B. A., Wooldridge, P. J., Jimenez, J. L., Campuzano-Jost, P., Day, D. A., Hu, W., Shepson, P. B., Xiong, F., Blake, D. R., Goldstein, A. H., Misztal, P. K., Hanisco, T. F., Wolfe, G. M., Ryerson, T. B., Wisthaler, A., and Mikoviny, T.: Organic nitrate chemistry and its implications for nitrogen budgets in an isoprene- and monoterpene-rich atmosphere: constraints from aircraft (SEAC(4)RS) and ground-based (SOAS) observations in the Southeast US, Atmos. Chem. Phys., 16, 5969-5991, https://doi.org/10.5194/acp-16-5969-2016, 2016.

Fry, J. L., Draper, D. C., Zarzana, K. J., Campuzano-Jost, P., Day, D. A., Jimenez, J. L., Brown, S. S., Cohen, R. C., Kaser, L., Hansel, A., Cappellin, L., Karl, T., Roux, A. H., Turnipseed, A., Cantrell, C., Lefer, B. L., and Grossberg, N.: Observations of gas- and aerosol-phase organic nitrates at BEACHON-RoMBAS 2011, Atmos. Chem. Phys., 13, 8585-8605, https://doi.org/10.5194/acp-13-8585-2013, 2013.

Gilman, J. B., Lerner, B. M., Kuster, W. C., Goldan, P. D., Warneke, C., Veres, P. R., Roberts, J. M., de Gouw, J. A., Burling, I. R., and Yokelson, R. J.: Biomass burning emissions and potential air quality impacts of volatile organic compounds and other trace gases from fuels common in the US, Atmos. Chem. Phys., 15, 13915-13938, https://doi.org/10.5194/acp-15-13915-2015, 2015.

Hamilton, J. F., Bryant, D. J., Edwards, P. M., Ouyang, B., Bannan, T. J., Mehra, A., Mayhew, A. W., Hopkins, J. R., Dunmore, R. E., Squires, F. A., Lee, J. D., Newland, M. J., Worrall, S. D., Bacak, A., Coe, H., Percival, C., Whalley, L. K., Heard, D. E., Slater, E. J., Jones, R. L., Cui, T., Surratt, J. D., Reeves, C. E., Mills, G. P., Grimmond, S., Sun, Y., Xu, W., Shi, Z., and Rickard, A. R.: Key Role of NO3 Radicals in the Production of Isoprene Nitrates and Nitrooxyorganosulfates in Beijing, Environ. Sci. Technol., 55, 842-853, https://doi.org/10.1021/acs.est.0c05689, 2021.

Hao, L. Q., Kortelainen, A., Romakkaniemi, S., Portin, H., Jaatinen, A., Leskinen, A., Komppula, M., Miettinen, P., Sueper, D., Pajunoja, A., Smith, J. N., Lehtinen, K. E. J., Worsnop, D. R., Laaksonen, A., and Virtanen, A.: Atmospheric submicron aerosol composition and particulate organic nitrate formation in a boreal forestland–urban mixed region, Atmos. Chem. Phys., 14, 13483-13495, https://doi.org/10.5194/acp-14-13483-2014, 2014.

Hayes, P. L., Ortega, A. M., Cubison, M. J., Froyd, K. D., Zhao, Y., Cliff, S. S., Hu, W. W., Toohey, D. W., Flynn, J. H., Lefer, B. L., Grossberg, N., Alvarez, S., Rappenglück, B., Taylor, J. W., Allan, J. D., Holloway, J. S., Gilman, J. B., Kuster, W. C., de Gouw, J. A., Massoli, P., Zhang, X., Liu, J., Weber, R. J., Corrigan, A. L., Russell, L. M., Isaacman, G., Worton, D. R., Kreisberg, N. M., Goldstein, A. H., Thalman, R., Waxman, E. M., Volkamer, R., Lin, Y. H., Surratt, J. D., Kleindienst, T. E., Offenberg, J. H., Dusanter, S., Griffith, S., Stevens, P. S., Brioude, J., Angevine, W. M., and Jimenez, J. L.: Organic aerosol composition and sources in Pasadena, California, during the 2010 CalNex campaign, J. Geophys. Res.: Atmos., 118, 9233-9257, 10.1002/jgrd.50530, 2013.

Herndon, S. C., Onasch, T. B., Wood, E. C., Kroll, J. H., Canagaratna, M. R., Jayne, J. T., Zavala, M. A., Knighton, W. B., Mazzoleni, C., Dubey, M. K., Ulbrich, I. M., Jimenez, J. L., Seila, R., de Gouw, J. A., de Foy, B., Fast, J., Molina, L. T., Kolb, C. E., and Worsnop, D. R.: Correlation of secondary organic aerosol with odd oxygen in Mexico City, Geophys. Res. Lett., 35, https://doi.org/10.1029/2008GL034058, 2008.

Hilas, C. S., Goudos, S. K., and Sahalos, J. N.: Seasonal decomposition and forecasting of telecommunication data: A comparative case study, Technological Forecasting and Social Change, 73, 495-509, https://doi.org/10.1016/j.techfore.2005.07.002, 2006.

Ho, K. F., Engling, G., Ho, S. S. H., Huang, R., Lai, S., Cao, J., and Lee, S. C.: Seasonal variations of anhydrosugars in PM2.5 in the Pearl River Delta Region, China, Tellus B: Chemical and Physical Meteorology, 66, 10.3402/tellusb.v66.22577, 2014.

Hu, W., Hu, M., Hu, W., Jimenez, J. L., Yuan, B., Chen, W., Wang, M., Wu, Y., Chen, C., Wang, Z., Peng, J., Zeng, L., and Shao, M.: Chemical composition, sources, and aging process of submicron aerosols in Beijing: Contrast between summer and winter, J. Geophys. Res.: Atmos., 121, 1955-1977, 10.1002/2015jd024020, 2016.

Huang, W., Saathoff, H., Shen, X., Ramisetty, R., Leisner, T., and Mohr, C.: Chemical Characterization of Highly Functionalized Organonitrates Contributing to Night-Time Organic Aerosol Mass Loadings and Particle Growth, Environ. Sci. Technol., 53, 1165-1174, https://doi.org/10.1021/acs.est.8b05826, 2019.

Isaacman-VanWertz, G., Massoli, P., O'Brien, R., Lim, C., Franklin, J. P., Moss, J. A., Hunter, J. F., Nowak, J. B., Canagaratna, M. R., Misztal, P. K., Arata, C., Roscioli, J. R., Herndon, S. T., Onasch, T. B., Lambe, A. T., Jayne, J. T., Su, L., Knopf, D. A., Goldstein, A. H., Worsnop, D. R., and Kroll, J. H.: Chemical evolution of atmospheric organic carbon over multiple generations of oxidation, Nature Chemistry, 10, 462-468, https://doi.org/10.1038/s41557-018-0002-2, 2018.

Iyer, S., Lopez-Hilfiker, F., Lee, B. H., Thornton, J. A., and Kurtén, T.: Modeling the Detection of Organic and Inorganic Compounds Using Iodide-Based Chemical Ionization, The Journal of Physical Chemistry A, 120, 576-587, https://doi.org/10.1021/acs.jpca.5b09837, 2016.

Jiang, F., Liu, J., Cheng, Z., Ding, P., Zhu, S., Yuan, X., Chen, W., Zhang, Z., Zong, Z., Tian, C., Hu, W., Zheng, J., Szidat, S., Li, J., and Zhang, G.: Quantitative evaluation for the sources and aging processes of organic aerosols in urban Guangzhou: Insights from a comprehensive method of dual-carbon isotopes and macro tracers, Sci Total Environ, 164182, https://doi.org/10.1016/j.scitotenv.2023.164182, 2023.

Kiendler-Scharr, A., Mensah, A. A., Friese, E., Topping, D., Nemitz, E., Prevot, A. S. H., Äijälä, M., Allan, J., Canonaco, F., Canagaratna, M., Carbone, S., Crippa, M., Dall Osto, M., Day, D. A., De Carlo, P., Di Marco, C. F., Elbern, H., Eriksson, A., Freney, E., Hao, L., Herrmann, H., Hildebrandt, L., Hillamo, R., Jimenez, J. L., Laaksonen, A., McFiggans, G., Mohr, C., O'Dowd, C., Otjes, R., Ovadnevaite, J., Pandis, S. N., Poulain, L., Schlag, P., Sellegri, K., Swietlicki, E., Tiitta, P., Vermeulen, A., Wahner, A., Worsnop, D., and Wu, H. C.: Ubiquity of organic nitrates from nighttime chemistry in the European submicron aerosol, Geophys. Res. Lett., 43, 7735-7744, https://doi.org/10.1002/2016gl069239, 2016.

Lanz, V. A., Prévôt, A. S. H., Alfarra, M. R., Weimer, S., Mohr, C., DeCarlo, P. F., Gianini, M. F. D., Hueglin, C., Schneider, J., Favez, O., D'Anna, B., George, C., and Baltensperger, U.: Characterization of aerosol chemical composition with aerosol mass spectrometry in Central Europe: an overview, Atmos. Chem. Phys., 10, 10453-10471, https://doi.org/10.5194/acp-10-10453-2010, 2010.

Lee, A. K. Y., Adam, M. G., Liggio, J., Li, S.-M., Li, K., Willis, M. D., Abbatt, J. P. D., Tokarek, T. W., Odame-Ankrah, C. A., Osthoff, H. D., Strawbridge, K., and Brook, J. R.: A large contribution of anthropogenic organo-nitrates to secondary organic aerosol in the Alberta oil sands, Atmos. Chem. Phys., 19, 12209-12219, https://doi.org/10.5194/acp-19-12209-2019, 2019.

Lee, B. H., Lopez-Hilfiker, F. D., D'Ambro, E. L., Zhou, P., Boy, M., Petäjä, T., Hao, L., Virtanen, A., and Thornton, J. A.: Semi-volatile and highly oxygenated gaseous and particulate organic compounds observed above a boreal forest canopy, Atmos. Chem. Phys., 18, 11547-11562, https://doi.org/10.5194/acp-18-11547-2018, 2018.

Lee, B. H., Mohr, C., Lopez-Hilfiker, F. D., Lutz, A., Hallquist, M., Lee, L., Romer, P., Cohen, R. C., Iyer, S., Kurten, T., Hu, W., Day, D. A., Campuzano-Jost, P., Jimenez, J. L., Xu, L., Ng, N. L., Guo, H., Weber, R. J., Wild, R. J., Brown, S. S., Koss, A., de Gouw, J., Olson, K., Goldstein, A. H., Seco, R., Kim, S., McAvey, K., Shepson, P. B., Starn, T., Baumann, K., Edgerton, E. S., Liu, J., Shilling, J. E., Miller, D. O., Brune, W., Schobesberger, S., D'Ambro, E. L., and Thornton, J. A.: Highly functionalized organic nitrates in the southeast United States: Contribution to secondary organic aerosol and reactive nitrogen budgets, Proc. Natl. Acad. Sci. U. S. A., 113, 1516-1521, https://doi.org/10.1073/pnas.1508108113, 2016.

Li, C., Wang, H., Chen, X., Zhai, T., Ma, X., Yang, X., Chen, S., Li, X., Zeng, L., and Lu, K.: Observation and modeling of organic nitrates on a suburban site in southwest China, Sci. Total Environ., 859, 160287, https://doi.org/10.1016/j.scitotenv.2022.160287, 2023.

Liebmann, J., Sobanski, N., Schuladen, J., Karu, E., Hellén, H., Hakola, H., Zha, Q., Ehn, M., Riva, M., Heikkinen, L., Williams, J., Fischer, H., Lelieveld, J., and Crowley, J. N.: Alkyl nitrates in the boreal forest: formation via the NO3-, OH- and O3 induced oxidation of biogenic volatile organic compounds and ambient lifetimes, Atmos. Chem. Phys., 19, 10391-10403, https://doi.org/10.5194/acp-19-10391-2019, 2019.

Liu, X., Huey, L. G., Yokelson, R. J., Selimovic, V., Simpson, I. J., Müller, M., Jimenez, J. L., Campuzano-Jost, P., Beyersdorf, A. J., Blake, D. R., Butterfield, Z., Choi, Y., Crounse, J. D., Day, D. A., Diskin, G. S., Dubey, M. K., Fortner, E., Hanisco, T. F., Hu, W., King, L. E., Kleinman, L., Meinardi, S., Mikoviny, T., Onasch, T. B., Palm, B. B., Peischl, J., Pollack, I. B., Ryerson, T. B., Sachse, G. W., Sedlacek, A. J., Shilling, J. E., Springston, S., St. Clair, J. M., Tanner, D. J., Teng, A. P., Wennberg, P. O., Wisthaler, A., and Wolfe, G. M.: Airborne measurements of western U.S. wildfire emissions: Comparison with prescribed burning and air quality implications, J. Geophys. Res.: Atmos., 122, 6108-6129, https://doi.org/10.1002/2016jd026315, 2017.

Lopez-Hilfiker, F. D., Iyer, S., Mohr, C., Lee, B. H., D'Ambro, E. L., Kurtén, T., and Thornton, J. A.: Constraining the sensitivity of iodide adduct chemical ionization mass spectrometry to multifunctional organic molecules using the collision limit and thermodynamic stability of iodide ion adducts, Atmos. Meas. Tech., 9, 1505-1512, https://doi.org/10.5194/amt-9-1505-2016, 2016.

Mao, S., Li, J., Cheng, Z., Zhong, G., Li, K., Liu, X., and Zhang, G.: Contribution of Biomass Burning to Ambient Particulate Polycyclic Aromatic Hydrocarbons at a Regional Background Site in East China, Environmental Science & Technology Letters, 5, 56-61, 10.1021/acs.estlett.8b00001, 2018.

Müller, S., Giorio, C., and Borduas-Dedekind, N.: Tracking the Photomineralization Mechanism in Irradiated Lab-Generated and Field-Collected Brown Carbon Samples and Its Effect on Cloud Condensation Nuclei Abilities, ACS Environmental Au, 10.1021/acsenvironau.2c00055, 2023.

Nault, B. A., Jo, D. S., McDonald, B. C., Campuzano-Jost, P., Day, D. A., Hu, W., Schroder, J. C., Allan, J., Blake, D. R., Canagaratna, M. R., Coe, H., Coggon, M. M., DeCarlo, P. F., Diskin, G. S., Dunmore, R., Flocke, F., Fried, A., Gilman, J. B., Gkatzelis, G., Hamilton, J. F., Hanisco, T. F., Hayes, P. L., Henze, D. K., Hodzic, A., Hopkins, J., Hu, M., Huey, L. G., Jobson, B. T., Kuster, W. C., Lewis, A., Li, M., Liao, J., Nawaz, M. O., Pollack, I. B., Peischl, J., Rappenglück, B., Reeves, C. E., Richter, D., Roberts, J. M., Ryerson, T. B., Shao, M., Sommers, J. M., Walega, J., Warneke, C., Weibring, P., Wolfe, G. M., Young, D. E., Yuan, B., Zhang, Q., de Gouw, J. A., and Jimenez, J. L.: Secondary organic aerosols from anthropogenic volatile organic compounds contribute substantially to air pollution mortality, Atmos. Chem. Phys., 21, 11201-11224, 10.5194/acp-21-11201-2021, 2021.

Perring, A. E., Pusede, S. E., and Cohen, R. C.: An observational perspective on the atmospheric impacts of alkyl and multifunctional nitrates on ozone and secondary organic aerosol, Chem. Rev., 113, 5848-5870, https://doi.org/10.1021/cr300520x, 2013.

Pye, H. O., Luecken, D. J., Xu, L., Boyd, C. M., Ng, N. L., Baker, K. R., Ayres, B. R., Bash, J. O., Baumann, K., Carter, W. P., Edgerton, E., Fry, J. L., Hutzell, W. T., Schwede, D. B., and Shepson, P. B.: Modeling the Current and Future Roles of Particulate Organic Nitrates in the Southeastern United States, Environ. Sci. Technol., 49, 14195-14203, https://doi.org/10.1021/acs.est.5b03738, 2015.

Robinson, M. A., Neuman, J. A., Huey, L. G., Roberts, J. M., Brown, S. S., and Veres, P. R.: Temperature-dependent sensitivity of iodide chemical ionization mass spectrometers, Atmos. Meas. Tech., 15, 4295-4305, https://doi.org/10.5194/amt-15-4295-2022, 2022.

Rollins, A. W., Browne, E. C., Min, K. E., Pusede, S. E., Wooldridge, P. J., Gentner, D. R., Goldstein, A. H., Liu, S., Day, D. A., Russell, L. M., and Cohen, R. C.: Evidence for NO(x) control over nighttime SOA formation, Science, 337, 1210-1212, https://doi.org/10.1126/science.1221520, 2012.

Salvador, C. M., Chou, C. C. K., Cheung, H. C., Ho, T. T., Tsai, C. Y., Tsao, T. M., Tsai, M. J., and Su, T. C.: Measurements of submicron organonitrate particles: Implications for the impacts of NOx pollution in a subtropical forest, Atmospheric Research, 245, https://doi.org/10.1016/j.atmosres.2020.105080, 2020.

Singla, V., Mukherjee, S., Pandithurai, G., Dani, K. K., and Safai, P. D.: Evidence of Organonitrate Formation at a High Altitude Site, Mahabaleshwar, during the Pre-monsoon Season, Aerosol and Air Quality Research, 19, 1241-1251, https://doi.org/10.4209/aaqr.2018.03.0110, 2019.

Sobanski, N., Thieser, J., Schuladen, J., Sauvage, C., Song, W., Williams, J., Lelieveld, J., and Crowley, J. N.: Day and night-time formation of organic nitrates at a forested mountain site in south-west Germany, Atmos. Chem. Phys., 17, 4115-4130, https://doi.org/10.5194/acp-17-4115-2017, 2017.

Takeuchi, M. and Ng, N. L.: Chemical composition and hydrolysis of organic nitrate aerosol formed from hydroxyl and nitrate radical oxidation of α-pinene and β-pinene, Atmos. Chem. Phys., 19, 12749-12766, https://doi.org/10.5194/acp-19-12749-2019, 2019.

Urban, R. C., Lima-Souza, M., Caetano-Silva, L., Queiroz, M. E. C., Nogueira, R. F. P., Allen, A. G., Cardoso, A. A., Held, G., and Campos, M. L. A. M.: Use of levoglucosan, potassium, and water-soluble organic carbon to characterize the origins of biomass-burning aerosols, Atmos. Environ., 61, 562-569, https://doi.org/10.1016/j.atmosenv.2012.07.082, 2012.

Wang, X., Shen, Z., Liu, F., Lu, D., Tao, J., Lei, Y., Zhang, Q., Zeng, Y., Xu, H., Wu, Y., Zhang, R., and Cao, J.: Saccharides in summer and winter PM2.5 over Xi'an, Northwestern China: Sources, and yearly variations of biomass burning contribution to PM2.5, Atmospheric Research, 214, 410-417, 10.1016/j.atmosres.2018.08.024, 2018.

Wang, Y., Hu, M., Lin, P., Guo, Q., Wu, Z., Li, M., Zeng, L., Song, Y., Zeng, L., Wu, Y., Guo, S., Huang, X., and He, L.: Molecular Characterization of Nitrogen-Containing Organic Compounds in Humic-like Substances Emitted from Straw Residue Burning, Environ. Sci. Technol., 51, 5951-5961, https://doi.org/10.1021/acs.est.7b00248, 2017.

Wood, E. C., Canagaratna, M. R., Herndon, S. C., Onasch, T. B., Kolb, C. E., Worsnop, D. R., Kroll, J. H., Knighton, W. B., Seila, R., Zavala, M., Molina, L. T., DeCarlo, P. F., Jimenez, J. L., Weinheimer, A. J., Knapp, D. J., Jobson, B. T., Stutz, J., Kuster, W. C., and Williams, E. J.: Investigation of the correlation between odd oxygen and secondary organic aerosol in Mexico City and Houston, Atmos. Chem. Phys., 10, 8947-8968, 10.5194/acp-10-8947-2010, 2010.

Xu, L., Suresh, S., Guo, H., Weber, R. J., and Ng, N. L.: Aerosol characterization over the southeastern United States using high-resolution aerosol mass spectrometry: spatial and seasonal variation of aerosol composition and sources with a focus on organic nitrates, Atmos. Chem. Phys., 15, 7307-7336, https://doi.org/10.5194/acp-15-7307-2015, 2015.

Xu, L., Crounse, J. D., Vasquez, K. T., Allen, H., Wennberg, P. O., Bourgeois, I., Brown, S. S., Campuzano-Jost, P., Coggon, M. M., Crawford, J. H., DiGangi, J. P., Diskin, G. S., Fried, A., Gargulinski, E. M., Gilman, J. B., Gkatzelis, G.

I., Guo, H., Hair, J. W., Hall, S. R., Halliday, H. A., Hanisco, T. F., Hannun, R. A., Holmes, C. D., Huey, L. G., Jimenez, J. L., Lamplugh, A., Lee, Y. R., Liao, J., Lindaas, J., Neuman, J. A., Nowak, J. B., Peischl, J., Peterson, D. A., Piel, F., Richter, D., Rickly, P. S., Robinson, M. A., Rollins, A. W., Ryerson, T. B., Sekimoto, K., Selimovic, V., Shingler, T., Soja, A. J., St. Clair, J. M., Tanner, D. J., Ullmann, K., Veres, P. R., Walega, J., Warneke, C., Washenfelder, R. A., Weibring, P., Wisthaler, A., Wolfe, G. M., Womack, C. C., and Yokelson, R. J.: Ozone chemistry in western U.S. wildfire plumes, Sci. Adv., 7, eabl3648, https://doi.org/10.1126/sciadv.abl3648, 2021a.

Xu, W., Takeuchi, M., Chen, C., Qiu, Y., Xie, C., Xu, W., Ma, N., Worsnop, D. R., Ng, N. L., and Sun, Y.: Estimation of particulate organic nitrates from thermodenuder–aerosol mass spectrometer measurements in the North China Plain, Atmos. Meas. Tech., 14, 3693-3705, https://doi.org/10.5194/amt-14-3693-2021, 2021b.

Xu, W., Han, T., Du, W., Wang, Q., Chen, C., Zhao, J., Zhang, Y., Li, J., Fu, P., Wang, Z., Worsnop, D. R., and Sun, Y.: Effects of Aqueous-Phase and Photochemical Processing on Secondary Organic Aerosol Formation and Evolution in Beijing, China, Environ. Sci. Technol., 51, 762-770, 10.1021/acs.est.6b04498, 2017.

Ye, C., Yuan, B., Lin, Y., Wang, Z., Hu, W., Li, T., Chen, W., Wu, C., Wang, C., Huang, S., Qi, J., Wang, B., Wang, C., Song, W., Wang, X., Zheng, E., Krechmer, J. E., Ye, P., Zhang, Z., Wang, X., Worsnop, D. R., and Shao, M.: Chemical characterization of oxygenated organic compounds in the gas phase and particle phase using iodide CIMS with FIGAERO in urban air, Atmos. Chem. Phys., 21, 8455-8478, https://doi.org/10.5194/acp-21-8455-2021, 2021.

Yu, K., Zhu, Q., Du, K., and Huang, X.-F.: Characterization of nighttime formation of particulate organic nitrates based on high-resolution aerosol mass spectrometry in an urban atmosphere in China, Atmos. Chem. Phys., 19, 5235-5249, https://doi.org/10.5194/acp-19-5235-2019, 2019.

Zhan, B., Zhong, H., Chen, H., Chen, Y., Li, X., Wang, L., Wang, X., Mu, Y., Huang, R.-J., George, C., and Chen, J.: The roles of aqueous-phase chemistry and photochemical oxidation in oxygenated organic aerosols formation, Atmos. Environ., 266, 118738, https://doi.org/10.1016/j.atmosenv.2021.118738, 2021.

Zhang, C., Lu, X., Zhai, J., Chen, H., Yang, X., Zhang, Q., Zhao, Q., Fu, Q., Sha, F., and Jin, J.: Insights into the formation of secondary organic carbon in the summertime in urban Shanghai, JEnvS, 72, 118-132, https://doi.org/10.1016/j.jes.2017.12.018, 2018.

Zhu, H.-X., Tao, X.-M., Wang, C., Zhang, L.-L., and Zheng, X.-Y.: Spatial and Temporal Distribution Characteristics of Levoglucosan and Its Isomers in PM2.5 in Beijing and Six Surrounding Cities, Environmental Science, 41, 1544-1549, 10.13227/j.hjkx.201906029, 2020.

Response of "The Important Contribution of Secondary Formation and Biomass Burning to Oxidized Organic Nitrogen (OON) in a Polluted Urban Area: Insights from In Situ FIGAERO-CIMS Measurements" in *Atmos. Chem. Phys. Discuss. Doi: 10.5194/acp-2023-8*

Anonymous Referee #2

2.0. The authors performed measurements of gas and particle-phase organic compounds using a FIGAERO-CIMS in a polluted urban location in China, with a particular focus in oxidized organic nitrogen species. Using $C_6H_{10}O_5$ (levoglucosan) as a tracer, they estimated the contribution of biomass burning to the measured gas and particle concentrations. Calculations were done to estimate the contribution of different oxidants and precursors to secondary organic nitrogen production. Broadly, the measurements and analysis presented in this manuscript are useful for helping to understand sources of organic nitrogen gases and particles in urban areas. Before this work is published, I believe there are several major issues that should be addressed. If I understand the experimental setup correctly, I am worried about the impact of sampling through a nafion tube. I think the authors should consider how much that could affect their measurements in light of recent literature on the topic. I also want to see an uncertainty analysis of the measurements, especially of the voltage scanning technique that is still a relatively new method of CIMS quantification. Taken together, I think the authors should carefully discuss the strengths or limits of their conclusions in the context of these uncertainties.

A2.0. We appreciate the reviewer for his/her insightful comments and suggestions, which help us tremendously in improving the quality of our work. Following the reviewer's suggestions, we have carefully revised the manuscript. To facilitate the review process, we have copied the reviewer comments in black text. Our responses are in regular blue font. We have responded to all the referee comments and made alterations to our paper **(in bold text).**

Comments:

2.1. Line 103: Have the authors investigated any artifacts that could result from sampling the CIMS through a nafion dryer? For instance, have you considered possible particle losses, or losses of compounds with particular functional groups that do not transmit well through nafion? This previous work from Liu et al. 2019 indicates that polar S/IVOCs do not

transmit well through nafion (https://amt.copernicus.org/articles/12/3137/2019/). This could be a critical problem for this work, and needs to be addressed.

A2.1: Thanks for the reviewer's comment. We need to point out that the nafion dryer was only set in the aerosol sampling line, not the gas phase line, thus the gas-phase S/IVOCs shall not be affected. The nafion dryer was necessary in our study due to the high humidity of ambient air (72 ± 17%), which could lead to the water condensation on the sampling filters of FIGAERO-CIMS under room temperatures. Liu et al. 2019 recommended that "Aerosols in equilibrium with S/IVOCs will be perturbed by the removal of the gases by the Nafion, so we recommend installing Nafion dryers or humidifiers at the last possible location before an instrument and to minimize residence time both in the dryer and between the dryer and instrument whenever possible." In our setup, we set up the nafion dryer around 1 meter ahead of the FIGAERO inlet at a flow rate of 5 L min^{-1} with 1/4-inch stainless tubes. The total residence time of aerosol in the dryer and between the dryer and instrument are ~ 0.12 and 0.23 second respectively. For this time scale, the removal of SVOCs would be around less than two percents based on partitioning delay model (Pagonis et al., 2017). Thus, we believe that the loss of SVOC in aerosol phases in such a short time shall be very small. Also, we added a reminder to the readers that accurate correction for the losses to nafion dryer remains impossible. No loss correction was performed in this study. To clarify this, we revised the relative discussion in line 105-112:

"The sampling flow rate is 3.8 L min^{-1} for gas sampling line and 5 L min^{-1} for particle line. A $PM_{2.5}$ cyclone inlet and a nafion dryer (Perma Pure, model PD-07018T-12MSS) were set ahead of the particle sampling inlet of the FIGAERO to keep the filter for aerosol sampling not getting wet due to the high ambient RH (72 ± 17%) in this campaign. Recent studies show that aerosol in equilibrium with semi-/intermediate-volatility organic compounds (S/IVOCs) will be perturbed by the removal of the gases by the nafion (Liu et al. 2019). However, in this study, the retention time for particles through the nafion dryer was ~0.12 s, which might lead to a very small change of S/IVOCs signal on such a timescale (< a few percents) based on the partitioning delay model (Pagonis et al., 2017). In addition, an accurate correction for S/IVOCs loss in nafion dryer is also not available in current (Liu et al. 2019). Thus, no S/IVOCs correction on aerosol phase was performed in this study."

2.2. Line 132: I have some questions about the CIMS calibration. I suggest the authors provide the calibrations factors that they determined for the 39 species that were calibrated. Calibrating a CIMS is challenging, but if the authors provide their calibration numbers, then readers can place the resulting concentrations in context of other measurements with possibly different calibration factors (each instrument can be different). I do not see these numbers in Ye et al. 2021 either, but maybe they are published somewhere.

A2.2: The calibration factors for the 39 species were provided in the excel file of the supplement zip package of Ye et al. (2021). We present the introduction picture and the calibration factors of the 39 species in the excel file as Figure A1 below. We also added sentences in line 147-148 to remind readers in the revised main text:

"Their calibration factors were shown in the excel file of the supplement zip package of Ye et al. (2021)."

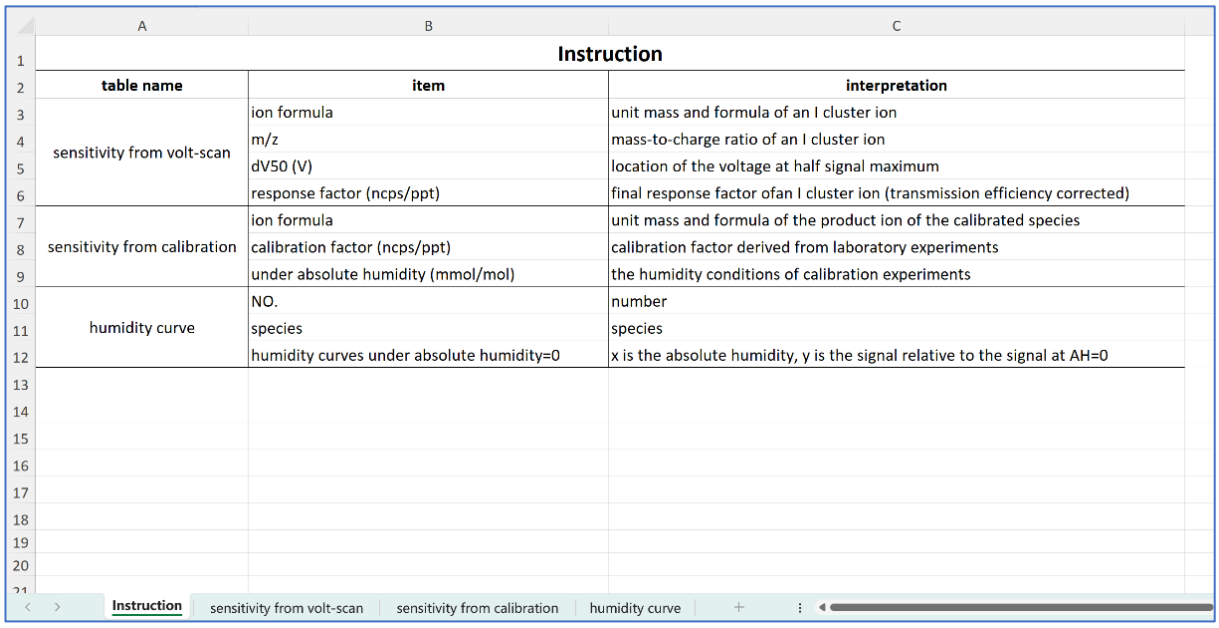

Instruction

table name	item	interpretation
sensitivity from volt-scan	ion formula	unit mass and formula of an I cluster ion
	m/z	mass-to-charge ratio of an I cluster ion
	dV50 (V)	location of the voltage at half signal maximum
	response factor (ncps/ppt)	final response factor ofan I cluster ion (transmission efficiency corrected)
sensitivity from calibration	ion formula	unit mass and formula of the product ion of the calibrated species
	calibration factor (ncps/ppt)	calibration factor derived from laboratory experiments
	under absolute humidity (mmol/mol)	the humidity conditions of calibration experiments
humidity curve	NO.	number
	species	species
	humidity curves under absolute humidity=0	x is the absolute humidity, y is the signal relative to the signal at AH=0

Instruction | sensitivity from volt-scan | sensitivity from calibration | humidity curve

ion formula	calibration factor (ncps/ppt)	ion formula	calibration factor (ncps/ppt)
m154_IHCN	0.18906	m245_IC4H6O4	165.0587159
m170_IHNCO	0.236	m249_IC4H10O4	14.30139688
m173_ICH2O2	3.715316071	m251_IC7H8O2	22.68495
m187_IC2H4O2	0.053299232	m259_IC5H8O4	44.36595871
m190_IHNO3	28.198	m266_IC6H5NO3	149.04625
m197_ICl2	52.7818	m273_IC6H10O4	12.27945699
m199_IC3H4O2	0.052397933	m279_C5H12IO5	30.66094196
m201_IC3H6O2	0.041353661	m282_IC6H5NO4	92.45548519
m203_IC2H4O3	3.026823	m287_IC7H12O4	48.98198813
m215_IC3H4O3	0.252149667	m289_IC6H10O5	60.11453097
m215_IC4H8O2	0.063134493	m303_C6H8IO6	15.23744638
m217_IC3H6O3	11.3528	m311_IC10H16O3	1.5005
m221_IC6H6O	0.08899	m311_IC6H4N2O5	79.08
m229_IC5H10O2	0.084410205	m315_IC9H16O4	32.56962241
m231_IC3H4O4	87.57454226	m329_C10H18IO4	6.899674479
m235_IC7H8O	0.054	m357_C12H22IO4	7.243826042
m235_IN2O5	16.495	m381_C10H22IO7	1.310960973
m237_IC6H6O2	38.68219875		

Figure A1. The introduction of the excel file and the calibration factors of the 39 species of the supplement zip package of Ye et al. (2021).

2.3. Line 134a: I also would like to see more information about how the voltage scanning procedure was done. I see that there is information given in Ye et al. 2021, but the reader of this paper would benefit from more information included here instead of having to search in other papers for it. Also, it is my understanding that the voltage scanning technique can have relatively high uncertainty.

A2.3: We thank the reviewer for the comment. As the reviewer suggested, we added more information of the voltage scanning method in line 149-160:

" Lopez-Hilfiker et al. (2016) and Iyer et al. (2016) have verified the connections among the binding energy of the iodide-adduct bond, the voltage dissociating iodide adducts and the sensitivity of corresponding species. The relationship between the voltage difference (*dV*) and signal fraction remaining of an iodide-molecule adduct is established by scanning the *dV* between the skimmer of the first quadrupole and the entrance to the second quadrupole ion guide of the mass spectrometer. This relationship curve of an individual iodide adduct can be fitted by a sigmoid function and yields two parameters: S_0, the relative signal at the weakest *dV* compared to the signal under operational *dV*; dV_{50}, the voltage at which half of the maximum signal is removed (i.e., half the adducts that could be formed are de-clustered). A sigmoidal fit was then applied to the results of all the iodide adducts. An empirical relationship between relative sensitivity ($1/S_0$) and dV_{50} of each ion (includes levoglucosan) based on average values of the entire campaign was obtained. By linking the relative sensitivity of levoglucosan with its absolute sensitivity based on the authentic standard, the absolute sensitivity of all the uncalibrated OON species was determined, after taking into account the relative transmission efficient of all the ions. The detailed data of these response factors can be found in the supporting information of Ye et al. (2021)."

About the question of relative high uncertainty of the voltage scanning method (Isaacman-Vanwertz et al., 2018; Bi et al., 2021). This approach was found to carry high uncertainties for individual analytes (0.5 to 1 order of magnitude) but represents a central tendency that can be used to estimate the sum of analytes with reasonable error (~30% differences between predicted and measured moles) (Bi et al., 2021). By comparing sensitivity factors if the three nitrogen-containing compounds (in the list of calibrated species) derived from the two methods, an underestimation of 32−56% for the sensitivity from the voltage scanning method was found compared to the method using authentic standard compounds (Figure S3). Finally, an average value of 47% was regarded as the representative uncertainty of the voltage scanning method and the total mass loading of uncalibrated species in this study. To clarify this, we added the description of uncertainty analysis of the voltage scanning method in line 160-168:

"Three OON species which are 4-nitrophenol ($C_6H_5NO_3$), 2,4-dinitrophenol ($C_6H_4N_2O_5$), and 4-nitrocatechol ($C_6H_5NO_4$) were calibrated in both authentic standards and voltage scanning methods. By comparing their sensitivity (Fig. S3), the uncertainty of the voltage scanning method can be roughly estimated. Detailed description of the calibration curves and the application of the calibration curve to estimate the sensitivity can

be refferred to the supporting information text of Ye et al. (2021). In general, the voltage scanning method underestimates (32−56%) the sensitivity of OON in this study compared to the values using the standard compounds as real. This uncertainty was comparable with 30% uncertainty of all analytes in Bi et al. (2021) and 60% uncertainty of total carbon in Isaacman-Vanwertz et al. (2018) measured by the Iodide-CIMS. Finally, an avergae underestimation of 47% on sensitivity was taken as the uncertainty of the whole OON mass loading in this study."

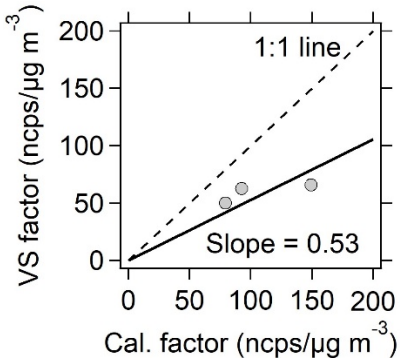

Figure S3. The scatterplot of calibration factors of three nitro-containing compounds (4-nitrophenol, 2,4-dinitrophenol, and 4-nitrocatechol) that derived from voltage scanning method and standard calibration. Based on the slope, 47% was regarded as the uncertainty of the voltage scanning method for OON calibration in this study. The detailed data can be found in the excel file of the supplement zip package of Ye et al. (2021).

2.4. Line 134b: When I look at Fig. S7c of Ye et al. 2021, the sensitivity values calculated from voltage scanning seem larger than I would expect. Perhaps this is normal for the instrument used here, and it would be useful to see the calibration numbers for more common compounds such as many of the 39 directly calibrated species (see my previous question).

A2.4: As the response in A2.2, we provided the calibration factor for all the OON ions used in this study by voltage scanning method and calibration factors of all 39 calibrated species in the excel file of the supplement zip package of Ye et al. (2021) and reminded the readers in line 158-159 in the maintext and caption of Fig. S3.

"The detailed data of these response factors can be found in the supporting information of Ye et al. (2021)."

2.5. Line 134c: My main comment about voltage scanning is that the authors should calculate the uncertainty for voltage scanning calibrations, and apply that uncertainty to the determination of gas and aerosol mass (especially organic nitrogen) measured by the CIMS. Section 3.1 compares AMS and CIMS masses in several ways, but I do not see any analysis of the uncertainties in calibration of the CIMS (or the AMS) and how that affects the comparison. In the Conclusions section Line 472, you say that the CIMS measured 28% of the total pOON, but how well do you know

that number? Is it possible that the CIMS actually measured a much larger fraction, but the calibrations are just really hard to do?

A2.5: Thank you for the reviewer's suggestion. As shown in the response A2.3 above, we added the analysis of uncertainty of the voltage scanning method by the comparison of three OON compounds that were calibrated in both methods. Finally, 47% was used for the OON detection in the CIMS measurement.

To assess the uncertainty of the comparison between the CIMS and the AMS, the error propagation law accounting for the uncertainties in both measurement techniques was applied. We added the detailed information on uncertainty estimation in Text S3. In addition, we revised the discussion of the comparison between CIMS and AMS in the section 3.1 and the conclusion section in the revised main text.

The uncertainty estimation added in Text S3:

"Uncertainty for the ratio of $pOrgNO_3$ measured by CIMS and AMS ($pOrgNO_{3,CIMS}$ vs $pOrgNO_{3,AMS}$). This uncertainty estimation was based on the Eq. (S8) below combined with error propagation law.

$$\frac{pOrgNO_{3,CIMS}}{pOrgNO_{3,AMS}} = \frac{pOON_{CIMS} \times \frac{MW_{[NO_3]}}{MW_{[pOON]}}}{pOrgNO_{3,AMS}} \qquad \textbf{(S8)}$$

The uncertainty of $pOON_{CIMS}$ was 47% according to the uncertainty of OON derived from the comparison of voltage scanning factors and calibration factors (Fig. S3), which was discussed in section 2.2.2 of the main text. The uncertainty of pOON molecular weight (MW, 234 ± 7.9 g mol^{-1}), which was obtained with CIMS measurement, was assigned to be 10%. The uncertainty of $pOrgNO_{3,AMS}$ was 30% which was obtained based on overall aerosol quantificaiton uncertainty of AMS (Salcedo et al., 2006). For OON quantification, the uncertainty of the NO_2^+/NO^+ ratio method was estimated using the lower and higher NO_2^+/NO^+ ratio from ONs (0.18 and 0.09) based on Xu et al. (2015), which was calculated to be 27% as discussed in Text S1. Finally, the total uncertainty of the pOON ratio between CIMS and AMS was 63%. It suggests that the $pOrgNO_{3,CIMS}$ can explain 28 ± 18% of $pOrgNO_{3,AMS}$."

The revised discussion of the comparison between the CIMS and the AMS in line 273-276:

"On the other side, if only $-ONO_2$/$-NO_2$ groups are considered to calculate pON_{CIMS} to be $pOrgNO_{3,CIMS}$, the calculated $pOrgNO_{3,CIMS}$ can explain 28 ± 18% of $pOrgNO_{3,AMS}$, which is consistent with the fraction (23%) of total functionalized OA detected using the CIMS versus total OA measured using the AMS (Ye et al., 2021).

The detailed analysis process on comparison uncertainty between AMS and CIMS can be found in Text S3 of the supporting information."

The revised conclusion section in line 526-528:

"The good comparison of pOON measured by AMS and FIGAERO-I-CIMS indicates that the CIMS can measure a fraction of 28 ± 18% of total pOON in this study."

2.6. Line 140: Instead of saying definitively that ONs were the dominant components of OON, I suggest you acknowledge the considerable uncertainty by saying something like this: "Some nitroaromatic signal may be detected as elemental formulas other than those listed above, and some of the signal at the elemental formulas identified here as nitroaromatic may have contributions from ON species. While uncertainty exists, it is likely that ONs dominated the OON observed during this campaign."

A2.6: We sincerely thank the reviewer for the comment and suggestion on revision. The original sentences were deleted. We added the revised sentences in line 172-175 of the main text suggested by the reviewer:

"**Some nitroaromatic signal may be detected as elemental formulas other than those listed above, and some of the signal at the elemental formulas identified here as nitroaromatics may have contribution from ON species. While uncertainty exists, it is likely that ONs dominated the OON observed during this campaign.**"

2.7. Line 148: How was this photochemical age determined? Even if it is described in the Chen et al 2021a citation, it would be useful to briefly describe here.

A2.7: The brief description of the determination of the photochemical age was added in line 184-187 of the revised main text:

"Multiple studies show that levoglucosan might be degraded due to photochemistry (Hennigan et al., 2010; Bai et al., 2013; Lai et al., 2014). We calculated the ambient photochemical age based on the ratios of two hydrocarbons (m+p-xylene and ethylbenzene) that react at different rates with OH radicals (Yuan et al., 2013; Wu et al., 2020; De Gouw et al., 2005). A daily average OH concentration of 1.5×10^6 molecule cm^{-3} was assumed here (Mao et al., 2009; Wang et al., 2020; Chen et al., 2021)."

2.8. Line 201: Since it makes more sense to compare the AMS pOrgNO3 with CIMS pOON when the AMS total nitrate is less than 5 ug m-3, I suggest you show remove the data points with greater than 5 ug m-3 from Fig. 1b. Then you

can keep Fig. S5a as it is to show all the data. Also, I am not sure I understand the purpose of Fig. S5b and you can probably remove it.

A2.8: We have updated Fig 1b and Fig S5b (now is Fig.S6 in the revised manuscript) as the reviewer suggested.

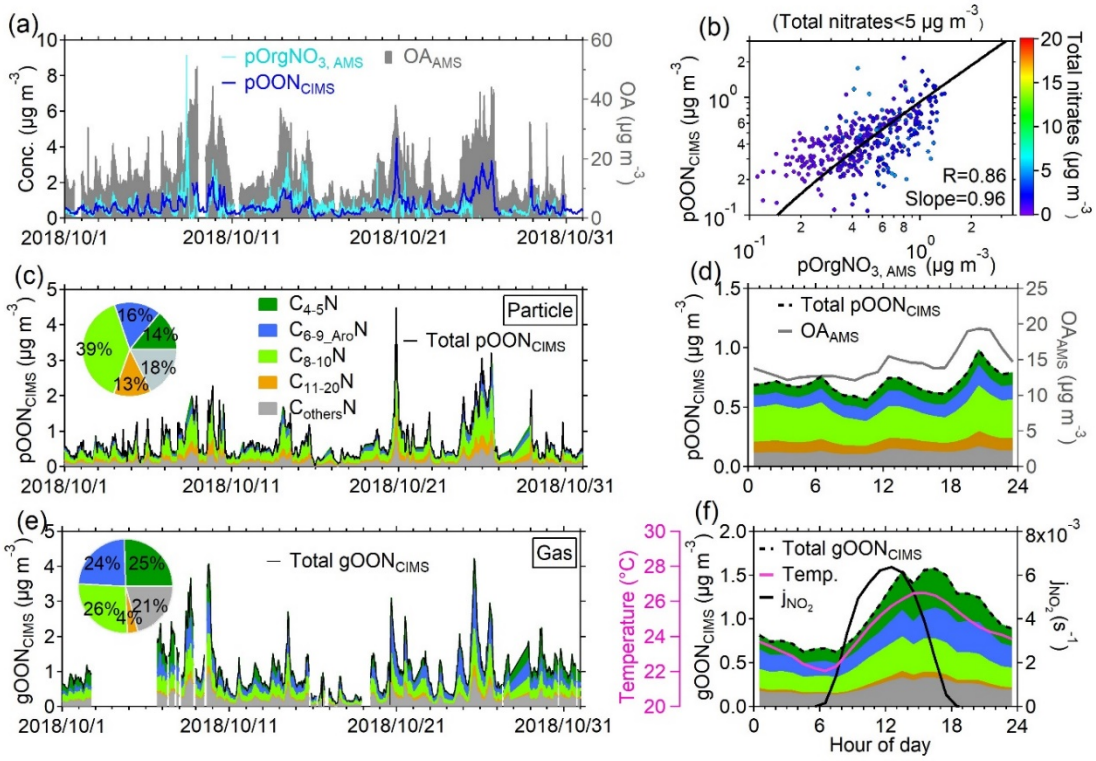

"Figure 1. Time series and variations of OON during the PRIDE-GBA campaign. (a) Time series of $pOON_{CIMS}$ and $pOrgNO_{3,\ AMS}$. Time series of total OA detected by the AMS is shown on the right axis. (b) Scatterplot of $pOON_{CIMS}$ versus $pOrgNO_{3,\ AMS}$ during the campaign. The term "total nitrates <5 μg m^{-3}" indicates the data used in this scatterplot is under the condition that the mass concentration of total nitrates (including organic nitrate and inorganic nitrate) measured by the AMS is lower than 5 μg m^{-3}. The points are color-coded using the total nitrate signals measured by the AMS. The scatterplot from all AMS and CIMS measurement can be found in Fig. S6. The logarithm was applied to both of the axes. Time series of (c) $pOON_{CIMS}$ and (e) $gOON_{CIMS}$, as well as the time series of their C_xN groups from the CIMS measurement. The insets show their average mass contributions to total $gOON_{CIMS}$ and $pOON_{CIMS}$ during the campaign, respectively. The average diurnal variations of (d) $pOON_{CIMS}$ and its C_xN groups, as well as OA; (f) Average diurnal variations of total $gOON_{CIMS}$ and its C_xN groups, photolysis rate of NO_2 (j_{NO2}), and temperature during the entire campaign. All the diurnal variations calculated throughout the manuscript are based on the average values. All the linear fitting are

based on the orthogonal distance regression (ODR) algorithm in this study. All the acronyms can be found in appendix A."

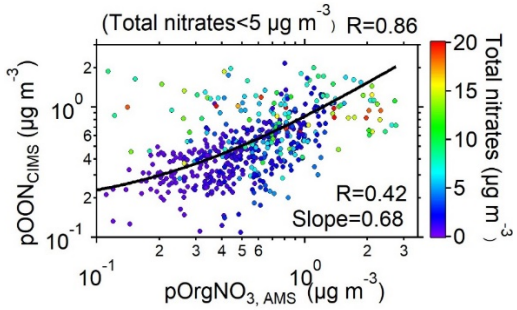

Figure S6. Scatterplot of $pOON_{CIMS}$ versus $pOrgNO_{3,\ AMS}$ during the campaign. The points are color-coded using total nitrates (including inorganic nitrate and organic nitrate) measured by AMS.

2.9. Fig. 2 Caption: The letters you use in the caption do not match the letters assigned to the figure panels. Please correct this.

A2.9: Corrected.

2.10. Line 278: I strongly recommend that when you refer to CIMS signals, that you always refer to the elemental formula rather than a specific isomer name. For instance, say C7H8O2 instead of methoxyphenol and C8H8O4 instead of vanillic acid. The iodide CIMS signal very likely comes from multiple isomers. Indeed, if you look at Fig. S12 of Palm et al. PNAS 2020, they show that the iodide CIMS signal at C7H8O2 is more likely to be methyl catechol rather than guaiacol. So here in the text, I would suggest changing to "Another two biomass burning tracers, i.e., C7H8O2 (methoxyphenol, methylcatechol, and isomers) and C8H8O4 (vanillic acid and isomers),…" You should also update the text when referring to C6H10O5 (levoglucosan and isomers) and anywhere else that is needed.

A2.10: We agree with the reviewer's suggestion. We updated all the "**levoglucosan**" to be "**$C_6H_{10}O_5$**" or "**$C_6H_{10}O_5$ (levoglucosan and its isomer)**" throughout the manuscript. We also revised all the CIMS signals with formula instead of compound names as suggested by the reviewer. I.e., $C_7H_8O_2$ (methoxyphenol, methylcatechol, and isomers), $C_8H_8O_4$ (vanillic acid and isomers) and $C_6H_5NO_3$ (nitrophenol and its isomers).

In addition, the GC-MS analysis based on filter-sampling was also applied to measure the isomers of levoglucosan, mannosan, and galactosan in this campaign, which was reported by Jiang et al. (2023). Based on the analysis, it was found that levoglucosan dominated the mass concentration in its three isomers (>90%), as shown in

Fig. A2 below. To clarify this, the information about the possible contribution of levoglucosan and its isomers to $C_6H_{10}O_5$ was updated in line 179-183:

"In the ambient air, the $C_6H_{10}O_5$ measured in the particle phase using the CIMS was probably composed by levoglucosan and its isomers (mannosan and galactosan) (Ye et al., 2021). The isomer measurement of $C_6H_{10}O_5$ in this campaign have revealed that the levoglucosan contributed 90 ± 2% mass loading of the three isomers of $C_6H_{10}O_5$ (Jiang et al., 2023), thus $C_6H_{10}O_5$ signal in this study can be used as a tracer for biomass burning emission (Bhattarai et al., 2019). The good correlation (R=0.78) between $C_6H_{10}O_5$ and another biomass burning tracer potassium (K^+) (Andreae, 1983; Wang et al., 2017), also supports this statement (Fig. S11a)."

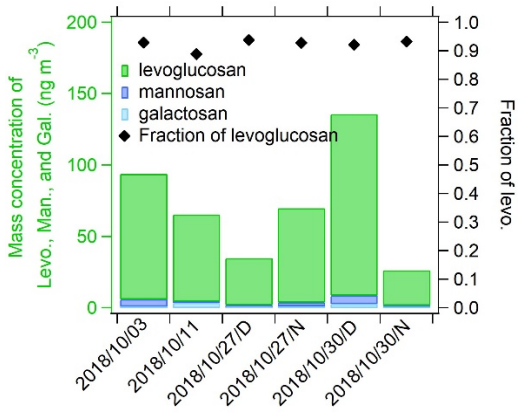

Figure A2. The mass concentration of $C_6H_{10}O_5$ isomers, i.e., levoglucosan, mannosan, and galactosan in this campaign. The mass fraction of levoglucosan to total $C_6H_{10}O_5$ isomer mass loading is also shown.

2.11. Table S1: Please indicate in the table caption that the data that was used to derive these slopes is also shown in Figs. S11 and S12.

A2.11: The caption of Table S1 was updated:

"Table S1. The regression slopes between measured gOON (pOON) vs particle-phase levoglucosan in selected biomass burning emission episodes. The data used to derive these slopes are also shown in Figs. S12 and S13. The average values based on different biomass burning episodes are also shown. "

2.12. Line 316: It seems reasonable to me that OON_bb would be an estimate of primary plus rapidly formed secondary OON from biomass burning emissions. I think that the OON_sec could also include slowly formed (i.e., next day) OON from biomass burning sources in addition to the other sources. That slowly formed OON would not correlate

with the primary C6H10O5 tracer. If the authors agree, please update the text. If not, do you have evidence to suggest otherwise?

A2.12: We agree with the reviewer's comment and updated the corresponding description in line 363-366 of the revised main text:

"the OON_{bb} herein is referred to as the total primary and rapidly formed secondary OON from biomass burning emissions. OON_{sec} is defined as secondary OON from non-biomass burning sources, e.g., biogenic and non-biomass burning anthropogenic sources and possible OON slowly formed from biomass burning sources (i.e., next day), which shall be minor."

2.13. Section 3.2: I would like to see a discussion at the end of (or throughout) this section of the authors' assessment of the uncertainties of this analysis. For instance, the iodide CIMS C6H10O5 signal is not a perfect representation of primary biomass burning emissions. That signal can have variability due to chemistry, variable emissions, etc. This should be discussed. Also I think a considerable source of uncertainty is that the OON_sec is defined just as the OON that is not biomass burning related, rather than defining OON_sec by some correlation with a secondary chemistry tracer. How could this affect your results?

A2.13: We thank the reviewer's comment. To assess the uncertainty of the calculation in section 3.2, we applied the Monte Carlo method to calculate the uncertainty for the fraction of biomass burning related OON to total OON. The calculation was repeated for 10000 times. In the calculation, the uncertainty of the ratio, $([OON_{measured}]/[levo.])_{bb}$, was derived from their uncertainty which was previously discussed in section 3.2. The uncertainty of the levoglucosan that was regarded as a tracer of biomass burning emissions was 10% considering the mass fraction among its isomers and its standard calibration (Ye et al., 2021), as shown in A2.10. In addition, we also include the standard deviation of source apportionment results at different time points in the final uncertainty calculation. The final results show that the biomass burning emissions accounted for 49 ± 23% of total pOON from CIMS, while the contribution was much lower (24 ± 25%) for gOON. To clarify this, we revised the description in line 372-376 of the main text and add the analysis of uncertainty in Text S3 in supporting information.

The revised section in line 375-378 of the main text:

"On average, biomass burning emissions accounted for 49 ± 23% of total pOON from CIMS, while the contribution was much lower (24 ± 25%) for gOON (Figs. 2b and 2d), indicating that biomass burning is one of the major sources for pOON measured by CIMS, and gOON is predominately from secondary formation

(76 ± 25%) (Huang et al., 2019; Lee et al., 2016). The uncertainty of these ratios representing the error of this source apportionment method, was estimated based on Monte Carlo method. The detailed calculation can be found in Text S3 of the supporting information."

The detailed uncertainty analysis added in Text S3 in supporting information:

"Uncertainty for the source apportionment of OON. Based on the Eq. (1−2), the uncertainty of the source apportionment of OON was estimated by Monte Carlo method with 10,000 calculations. The uncertainty of levoglucosan was 10% considering its standard calibration (Ye et al., 2021) and mass contribution (90 ± 2%) among isomers (referred to section 2.2.2). The uncertainty of the primary ratios of OON vs levoglucosan, $(([\mathbf{OON}_{\mathbf{measured}}]/[\mathbf{levo.}])_{\mathbf{bb}})$, was considered equal to their average standard deviation shown in Table S1, i.e., 20% and 42% for pOON and gOON, respectively. After performing the Monte Carlo method, the uncertainties of the OON_{bb} fraction in total OON were around 9% and 11% for aerosol and gas phase, respectively. The standard deviations of averaged OON_{bb} fraction in total OON from the entire campaign were around 22% and 23% for aerosol and gas phase, respectively. By combining the uncertainty from Monte Carlo and standard deviation due to averaging, the final contribution s with uncertainties of biomass burning to pOON and gOON are 49 ± 23% and 24 ±25%, respectively."

About the representativeness of levoglucosan itself as a tracer for biomass burning. We have addressed that the uncertainty might exist due to their photodegradation in the ambient air, as shown below in line 187-191. To account for the emission variability of levoglucosan, we selected the multiple plumes to obtain the primary ratio of OON with levoglucosan for minimizing the uncertainty. The primary ratio uncertainty was finally considered in the source apportionment results as shown above.

"The estimated results show that the average diurnal photochemical age varied from 0.2 days during the night to maximum 0.5 days in the daytime in this campaign (Chen et al., 2021), which was lower than the lifetime of levoglucosan (>1 day –26 days) determined in laboratory and field studies (Hennigan et al., 2010; Hoffmann et al., 2010; Lai et al., 2014; Bai et al., 2013; Bhattarai et al., 2019). It suggests that the levoglucosan observed in this study shall be stable for being the tracer of biomass burning emissions."

We understand the high uncertainty related to the OONsec due to its not being resolved based on secondary chemistry tracer. However, a very good correlation has been found between gas-phase secondary OON (gOONsec) and photooxidation product O_3, supporting its secondary origins. In addition, a good correlation between particle-

phase OONsec (pOONsec) and semi-volatile oxygenated OA (SV-OOA), which were freshly formed SOA, was also found, as shown in Figure S17 below. This also supports the pOONsec were from secondary sources. To clarify this, we added relative discussion and revised the sentence in line 372-374 in the revised main text:

"The particle-phase OON_{sec} also showed consistent variation (R=0.70) to semi-volatile oxygenated OA (SV-OOA), which was treated as freshly formed SOA during the day (Fig. S17) (Chen et al., 2021), supporting the secondary origins of $pOON_{sec}$. These results validated the source apportionment of OON applied herein."

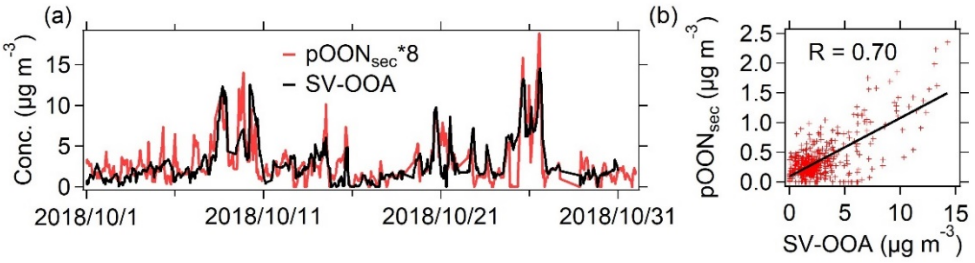

Figure S17. (a) The time series of pOONsec and semi-volatile oxygenated OA (SV-OOA) and (b) their scatterplot. The SV-OOA was treated as freshly formed secondary organic aerosol, which show good correlation with gas-phase oxidation product pentanones. The detailed information of SV-OOA can be found in Chen et al. (2021).

2.14. Line 458: This correlation of 0.52 < R < 0.79 is not very high, so I would not agree that this means that C10HxNOy (y>=6) "indeed mainly" comes from biomass burning emissions. Correlation does not mean causation, and Fig. 7b shows that these C10 compounds are present during the whole campaign and not just during biomass burning periods. I suggest the authors remove this assertion or follow it up with other analysis such as correlation with a monoterpene SOA tracer.

A2.14: We removed this assertion in the revised main text.

2.15. Line 472: I mentioned this in a comment earlier, but I would like to see what your estimated error bars number of how much pOON the CIMS sampled relative to the AMS. But, if this number is your best estimate, then how does this affect your conclusions? If the CIMS only measures a small fraction of the pOON, then is it justified to conclude that about half of pOON is from biomass burning, or can you really only say that about half of the 28% of measured pOON is from biomass burning emissions? There are some uncertainties here related to not being able to measure most of the organic nitrogen that I believe the authors should explore further.

A2.15: We thank the reviewer's comments and suggestions. As our response in the A2.5, the error bar for the fraction (28%) was 18% that was calculated by the uncertainty from pOON from the CIMS and the AMS. we revised the relative discussion in the conclusion section of the main text in line 526-530:

"The good comparison of pOON measured by AMS and FIGAERO-I-CIMS indicates that the CIMS can measure a fraction of 28 ± 18% of total pOON in this study. Compared to AMS, the missed pOON mass measured by CIMS is probably due to the lack of detection of less-polar OON (keto/alkyl ON) and/or non-nitrogen-containing pOON resulting from the loss of $-NO_2$ group by thermal desorption in CIMS measurement."

We agree with the reviewer that the source apportionment is only applicable to the pOON measured by CIMS and further work focused on the OON which was not detected by the CIMS should attract more attention. To clarify this, we revised the discussion in line 531-535:

"Using $C_6H_{10}O_5$ (~90% of levoglucosan) as the biomass burning tracer for source apportionment, almost half of the pOON measured by the CIMS is attributed to biomass burning in this study, underscoring the important contribution of biomass burning to pOON in this urban area. Biomass burning is a very common source across the world. The proposed estimation method in this study might help to clarify the exact biomass burning contribution to OON and their potential atmospheric implication. Note that the sources of the undetected pOON from CIMS are still unknown, which shall be further investigated. "

Reference

Andreae, M. O.: Soot Carbon and Excess Fine Potassium: Long-Range Transport of Combustion-Derived Aerosols, Science, 220, 1148-1151, https://doi.org/10.1126/science.220.4602.1148, 1983.

Bai, J., Sun, X., Zhang, C., Xu, Y., and Qi, C.: The OH-initiated atmospheric reaction mechanism and kinetics for levoglucosan emitted in biomass burning, Chemosphere, 93, 2004-2010, https://doi.org/10.1016/j.chemosphere.2013.07.021, 2013.

Bhattarai, H., Saikawa, E., Wan, X., Zhu, H., Ram, K., Gao, S., Kang, S., Zhang, Q., Zhang, Y., Wu, G., Wang, X., Kawamura, K., Fu, P., and Cong, Z.: Levoglucosan as a tracer of biomass burning: Recent progress and perspectives, Atmospheric Research, 220, 20-33, https://doi.org/10.1016/j.atmosres.2019.01.004, 2019.

Bi, C., Krechmer, J. E., Frazier, G. O., Xu, W., Lambe, A. T., Claflin, M. S., Lerner, B. M., Jayne, J. T., Worsnop, D. R., Canagaratna, M. R., and Isaacman-VanWertz, G.: Quantification of isomer-resolved iodide chemical ionization mass spectrometry sensitivity and uncertainty using a voltage-scanning approach, Atmos. Meas. Tech., 14, 6835-6850, https://doi.org/10.5194/amt-14-6835-2021, 2021.

Chen, W., Ye, Y. Q., Hu, W. W., Zhou, H. S., Pan, T. L., Wang, Y. K., Song, W., Song, Q. C., Ye, C. S., Wang, C. M., Wang, B. L., Huang, S., Yuan, B., Zhu, M., Lian, X. F., Zhang, G. H., Bi, X. H., Jiang, F., Liu, J. W., Canonaco, F., Prevot, A. S. H., Shao, M., and Wang, X. M.: Real-Time Characterization of Aerosol Compositions, Sources, and Aging Processes in Guangzhou During PRIDE-GBA 2018 Campaign, J. Geophys. Res.: Atmos., 126, e2021JD035114. , https://doi.org/10.1029/2021JD035114, 2021.

de Gouw, J. A., Warneke, C., Stohl, A., Holloway, J., Trainer, M., and Fehsenfeld, F. C.: Emissions and Photochemistry of Oxygenated VOCs in the Outflow from Urban Centers in the Northeastern U.S, 2005/12/1, A31E-05,

Hennigan, C. J., Sullivan, A. P., Collett, J. L., and Robinson, A. L.: Levoglucosan stability in biomass burning particles exposed to hydroxyl radicals, Geophys. Res. Lett., 37, n/a-n/a, https://doi.org/10.1029/2010gl043088, 2010.

Hoffmann, D., Tilgner, A., Iinuma, Y., and Herrmann, H.: Atmospheric Stability of Levoglucosan: A Detailed Laboratory and Modeling Study, Environ. Sci. Technol., 44, 694-699, https://doi.org/10.1021/es902476f, 2010.

Huang, W., Saathoff, H., Shen, X., Ramisetty, R., Leisner, T., and Mohr, C.: Chemical Characterization of Highly Functionalized Organonitrates Contributing to Night-Time Organic Aerosol Mass Loadings and Particle Growth, Environ. Sci. Technol., 53, 1165-1174, https://doi.org/10.1021/acs.est.8b05826, 2019.

Isaacman-VanWertz, G., Massoli, P., O'Brien, R., Lim, C., Franklin, J. P., Moss, J. A., Hunter, J. F., Nowak, J. B., Canagaratna, M. R., Misztal, P. K., Arata, C., Roscioli, J. R., Herndon, S. T., Onasch, T. B., Lambe, A. T., Jayne, J. T., Su, L., Knopf, D. A., Goldstein, A. H., Worsnop, D. R., and Kroll, J. H.: Chemical evolution of atmospheric organic carbon over multiple generations of oxidation, Nature Chemistry, 10, 462-468, https://doi.org/10.1038/s41557-018-0002-2, 2018.

Iyer, S., Lopez-Hilfiker, F., Lee, B. H., Thornton, J. A., and Kurtén, T.: Modeling the Detection of Organic and Inorganic Compounds Using Iodide-Based Chemical Ionization, The Journal of Physical Chemistry A, 120, 576-587, https://doi.org/10.1021/acs.jpca.5b09837, 2016.

Jiang, F., Liu, J., Cheng, Z., Ding, P., Zhu, S., Yuan, X., Chen, W., Zhang, Z., Zong, Z., Tian, C., Hu, W., Zheng, J., Szidat, S., Li, J., and Zhang, G.: Quantitative evaluation for the sources and aging processes of organic aerosols in urban Guangzhou: Insights from a comprehensive method of dual-carbon isotopes and macro tracers, Sci Total Environ, 164182, https://doi.org/10.1016/j.scitotenv.2023.164182, 2023.

Lai, C., Liu, Y., Ma, J., Ma, Q., and He, H.: Degradation kinetics of levoglucosan initiated by hydroxyl radical under different environmental conditions, Atmos. Environ., 91, 32-39, https://doi.org/10.1016/j.atmosenv.2014.03.054, 2014.

Lee, B. H., Mohr, C., Lopez-Hilfiker, F. D., Lutz, A., Hallquist, M., Lee, L., Romer, P., Cohen, R. C., Iyer, S., Kurten, T., Hu, W., Day, D. A., Campuzano-Jost, P., Jimenez, J. L., Xu, L., Ng, N. L., Guo, H., Weber, R. J., Wild, R. J., Brown, S.

S., Koss, A., de Gouw, J., Olson, K., Goldstein, A. H., Seco, R., Kim, S., McAvey, K., Shepson, P. B., Starn, T., Baumann, K., Edgerton, E. S., Liu, J., Shilling, J. E., Miller, D. O., Brune, W., Schobesberger, S., D'Ambro, E. L., and Thornton, J. A.: Highly functionalized organic nitrates in the southeast United States: Contribution to secondary organic aerosol and reactive nitrogen budgets, Proc. Natl. Acad. Sci. U. S. A., 113, 1516-1521, https://doi.org/10.1073/pnas.1508108113, 2016.

Lopez-Hilfiker, F. D., Iyer, S., Mohr, C., Lee, B. H., D'Ambro, E. L., Kurtén, T., and Thornton, J. A.: Constraining the sensitivity of iodide adduct chemical ionization mass spectrometry to multifunctional organic molecules using the collision limit and thermodynamic stability of iodide ion adducts, Atmos. Meas. Tech., 9, 1505-1512, https://doi.org/10.5194/amt-9-1505-2016, 2016.

Mao, J., Ren, X., Brune, W. H., Olson, J. R., Crawford, J. H., Fried, A., Huey, L. G., Cohen, R. C., Heikes, B., Singh, H. B., Blake, D. R., Sachse, G. W., Diskin, G. S., Hall, S. R., and Shetter, R. E.: Airborne measurement of OH reactivity during INTEX-B, Atmos. Chem. Phys., 9, 163-173, https://doi.org/10.5194/acp-9-163-2009, 2009.

Pagonis, D., Krechmer, J. E., de Gouw, J., Jimenez, J. L., and Ziemann, P. J.: Effects of gas–wall partitioning in Teflon tubing and instrumentation on time-resolved measurements of gas-phase organic compounds, Atmos. Meas. Tech., 10, 4687-4696, https://doi.org/10.5194/amt-10-4687-2017, 2017.

Salcedo, D., Onasch, T. B., Dzepina, K., Canagaratna, M. R., Zhang, Q., Huffman, J. A., DeCarlo, P. F., Jayne, J. T., Mortimer, P., Worsnop, D. R., Kolb, C. E., Johnson, K. S., Zuberi, B., Marr, L. C., Volkamer, R., Molina, L. T., Molina, M. J., Cardenas, B., Bernabé, R. M., Márquez, C., Gaffney, J. S., Marley, N. A., Laskin, A., Shutthanandan, V., Xie, Y., Brune, W., Lesher, R., Shirley, T., and Jimenez, J. L.: Characterization of ambient aerosols in Mexico City during the MCMA-2003 campaign with Aerosol Mass Spectrometry: results from the CENICA Supersite, Atmos. Chem. Phys., 6, 925-946, 10.5194/acp-6-925-2006, 2006.

Wang, Y., Hu, M., Lin, P., Guo, Q., Wu, Z., Li, M., Zeng, L., Song, Y., Zeng, L., Wu, Y., Guo, S., Huang, X., and He, L.: Molecular Characterization of Nitrogen-Containing Organic Compounds in Humic-like Substances Emitted from Straw Residue Burning, Environ. Sci. Technol., 51, 5951-5961, https://doi.org/10.1021/acs.est.7b00248, 2017.

Wang, Z., Yuan, B., Ye, C., Roberts, J., Wisthaler, A., Lin, Y., Li, T., Wu, C., Peng, Y., Wang, C., Wang, S., Yang, S., Wang, B., Qi, J., Wang, C., Song, W., Hu, W., Wang, X., Xu, W., Ma, N., Kuang, Y., Tao, J., Zhang, Z., Su, H., Cheng, Y., Wang, X., and Shao, M.: High Concentrations of Atmospheric Isocyanic Acid (HNCO) Produced from Secondary Sources in China, Environ. Sci. Technol., 54, 11818-11826, https://doi.org/10.1021/acs.est.0c02843, 2020.

Wu, C., Wang, C., Wang, S., Wang, W., Yuan, B., Qi, J., Wang, B., Wang, H., Wang, C., Song, W., Wang, X., Hu, W., Lou, S., Ye, C., Peng, Y., Wang, Z., Huangfu, Y., Xie, Y., Zhu, M., Zheng, J., Wang, X., Jiang, B., Zhang, Z., and Shao, M.: Measurement report: Important contributions of oxygenated compounds to emissions and chemistry of volatile organic compounds in urban air, Atmos. Chem. Phys., 20, 14769-14785, https://doi.org/10.5194/acp-20-14769-2020, 2020.

Ye, C., Yuan, B., Lin, Y., Wang, Z., Hu, W., Li, T., Chen, W., Wu, C., Wang, C., Huang, S., Qi, J., Wang, B., Wang, C., Song, W., Wang, X., Zheng, E., Krechmer, J. E., Ye, P., Zhang, Z., Wang, X., Worsnop, D. R., and Shao, M.: Chemical characterization of oxygenated organic compounds in the gas phase and particle phase using iodide CIMS with FIGAERO in urban air, Atmos. Chem. Phys., 21, 8455-8478, https://doi.org/10.5194/acp-21-8455-2021, 2021.

Yuan, B., Hu, W. W., Shao, M., Wang, M., Chen, W. T., Lu, S. H., Zeng, L. M., and Hu, M.: VOC emissions, evolutions and contributions to SOA formation at a receptor site in eastern China, Atmos. Chem. Phys., 13, 8815-8832, https://doi.org/10.5194/acp-13-8815-2013, 2013.